Science Advances

AAAS

advances.sciencemag.org/cgi/content/full/4/3/eaar2978/DC1

Supplementary Materials for

$^{15}N_4$-1,2,4,5-tetrazines as potential molecular tags: Integrating bioorthogonal chemistry with hyperpolarization and unearthing *para*-N_2

Junu Bae, Zijian Zhou, Thomas Theis, Warren S. Warren, Qiu Wang

Published 9 March 2018, *Sci. Adv.* **4**, eaar2978 (2018)
DOI: 10.1126/sciadv.aar2978

This PDF file includes:

1. Synthesis and cycloaddition reactions of 1,2,4,5-tetrazines

1.1. General Experimental Information

Material Information. All commercially available reagents and solvents were used as received (unless otherwise stated). Thin-layer chromatography (TLC) was performed using aluminum plates pre-coated with 0.25 mm of 230–400 mesh silica gel with a fluorescent indicator (254 nm). TLC plates were visualized by exposure to ultraviolet light and/or exposure to a solution of $KMnO_4$ and/or vanillin stain. Organic solutions were concentrated *in vacuo* using a rotary evaporator. Column chromatography was performed with silica gel (60 Å, standard grade).

Nuclear magnetic resonance spectra were recorded at ambient temperature (unless otherwise stated) on Bruker AM-360 MHz, Varian iNova 400 MHz, or Varian iNova 500 MHz spectrometers. NMR data are represented as follows: chemical shift, multiplicity, coupling constant, and integration. All values for proton chemical shifts (δ_H) are reported in parts per million and are referenced to the residual internal CHD_2OD (δ 3.31). All values for carbon chemical shifts (δ_C) are reported in parts per million and are referenced to the carbon resonances in $CDCl_3$ (δ 77.0) or CD_3OD (δ 49.0). All values for nitrogen chemical shifts (δ_N) are reported in parts per million and are referenced to an external standard of liquid NH_3 (δ 0.0); the reference point is calculated from the ratios of resonance frequencies following IUPAC recommendations.*(44)* Resonances are described as s (singlet), d (doublet), t (triplet), q (quartet), quint (quintet), and combinations thereof. Coupling constants (*J*) are given in *Hz* and rounded to the nearest 0.1.

High resolution mass spectra were recorded by either (1) the Mass Spectrometry Facility at the Department of Chemistry at Duke University using an Agilent 6224 TOF LC/MS instrument (denoted by LC/ESI) or (2) the Analytic Chemistry Core at the Nicholas School of the Environment at Duke University using an Agilent 7890B GC and 7200 QTOF instrument (denoted by GC/EI). High resolution *m*/*z* values are reported in Daltons, calculated to 4 decimal points from the molecular formula. All found values are within 5 ppm tolerance.

Infrared spectra were recorded on a ThermoScientific Nicolet 6700 FTIR equipped with a diamond ATR. Absorption maxima (ν_{max}) are described as s (strong), m (medium), w (weak), and br (broad) and are quoted in wavenumbers (cm^{-1}). Only selected peaks are reported.

1.2. Synthesis of 1,2,4,5-Tetrazines

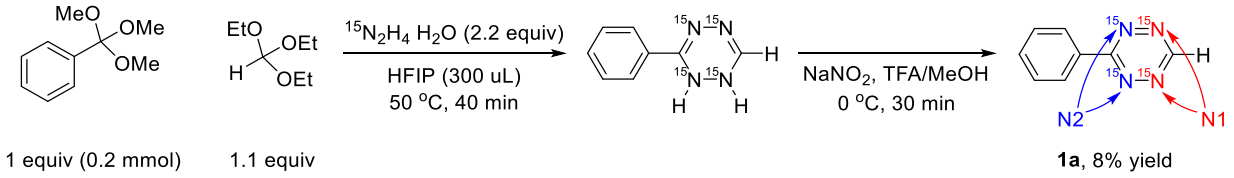

3-Phenyl-1,2,4,5-tetrazine-1,2,4,5-$^{15}N_4$ (1a). To a 1-dram vial, was added sequentially: trimethyl orthobenzoate (36.4 mg, 0.2 mmol, 1 equiv), hexafluoroisopropanol (300 µL), triethyl orthoformate (31.1 mg, 0.21 mmol, 1.05 equiv), and $^{15}N_2$-hydrazine hydrate (22.38 mg, 0.43 mmol, 2.15 equiv). The reaction mixture was stirred at 50°C for 40 min, then cooled to 0°C, followed by the addition of MeOH (300 µL) and $NaNO_2$ (41.4 mg, 0.6 mmol, 3.0 equiv). To this mixture, was added dropwise trifluoroacetic acid (300 µL) at 0°C, resulting in generation of a deep red color (CAUTION: toxic gas is generated at this step). The reaction mixture was stirred at 0°C for 30 min, and then was diluted with water (5 mL). The mixture was extracted with $CHCl_3$ (5 mL × 3). The organic layers were combined and concentrated *in vacuo*. Purification by column chromatography (pentane to 5% ethyl acetate–pentane) gave **1a** as a pink solid (2.5 mg, 8%). $\mathbf{R_f}$ = 0.82 (5% ethyl acetate–pentane); **^{1}H NMR** (360 MHz, CD_3OD): **δ** 10.34 (tt, $J_{H\text{-}N1}$ = 14.0, $J_{H\text{-}N2}$ = 2.4 Hz, 1H), 8.60–8.58 (m, 2H), 7.71–7.62 (m, 3H); **^{13}C NMR** (126 MHz, $CDCl_3$): **δ** 166.5–166.3 (m, 1C), 157.8–157.7 (m, 1C), 133.1, 131.6–131.5 (m, 1C), 129.3, 128.3; **^{15}N NMR** (36.5 MHz, CD_3OD): **δ** 389.4–388.3 (m, N1), 381.2–380.4 (m, N2); **FTIR** (thin film, CH_2Cl_2): 3359 (br), 2917, 1653 (br), 1407, 1260, 1015, 795 cm^{-1}; **HRMS-GC/EI** (m/z) Calc'd for ($C_8H_6{}^{15}N_4{}^+$) ($[M]^+$): 162.0468; found: 162.0473.

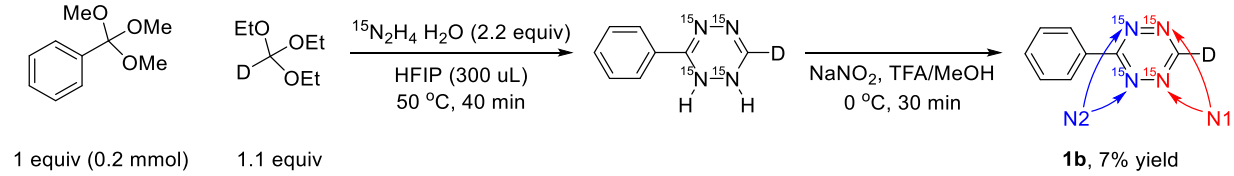

3-Phenyl-1,2,4,5-tetrazine-6-*d*-1,2,4,5-$^{15}N_4$ (1b). Following the same procedure for **1a**, substituting triethyl orthoformate-1-*d* (*45*) for triethyl orthoformate, **1b** was isolated as a pink solid (2.3 mg, 7%). $\mathbf{R_f}$ = 0.82 (5% ethyl acetate–pentane); **^{1}H NMR** (360 MHz, CD_3OD): **δ** 8.60–8.57 (m, 2H), 7.71–7.61 (m, 3H); **^{13}C NMR** (126 MHz, $CDCl_3$): **δ** 166.5, 157.9–157.2 (m, Csp^2–D), 133.1, 131.6, 129.4, 128.3; **^{15}N NMR** (36.5 MHz, CD_3OD): **δ** 389.0–388.2 (m, N1), 381.2–380.3 (m, N2); **FTIR** (thin film, CH_2Cl_2): 3356 (br), 2918, 1636 (br), 1407, 1264, 1113, 736 cm^{-1}; **HRMS-GC/EI** (m/z) Calc'd for ($C_8H_5D{}^{15}N_4{}^+$) ($[M]^+$): 163.0531; found: 163.0535.

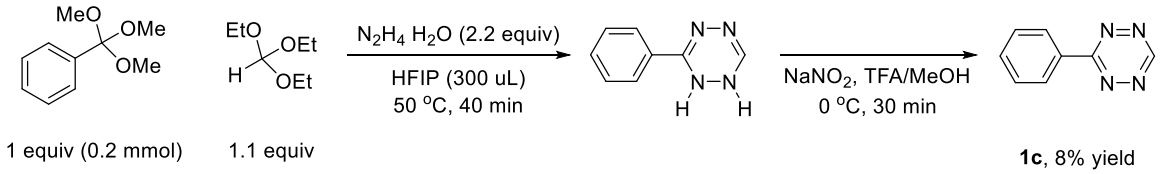

3-Phenyl-1,2,4,5-tetrazine (1c). Following the same procedure for **1a**, substituting natural abundance-hydrazine hydrate for $^{15}N_2$-hydrazine hydrate, **1c** was isolated as a pink solid (2.4 mg, 8%). $\mathbf{R_f}$ = 0.82 (5% ethyl acetate–pentane); **^{1}H NMR** (500 MHz, CD_3OD): **δ** 10.34 (s, 1H), 8.64–8.59 (m, 2H), 7.70–7.62 (m, 3H); **^{13}C NMR** (126 MHz, $CDCl_3$): **δ** 166.3, 157.7, 133.0, 131.5, 129.2, 128.1; **FTIR** (thin film, CH_2Cl_2): 3085, 2924, 1438, 1351, 914, 761, 689, 566 cm^{-1}; **HRMS-GC/EI** (m/z) Calc'd for ($C_8H_6N_4^+$) ([M]$^+$): 158.0587; found: 158.0593.

1.3. Cycloaddition Reactions of 1,2,4,5-Tetrazine/Cyclooctyne

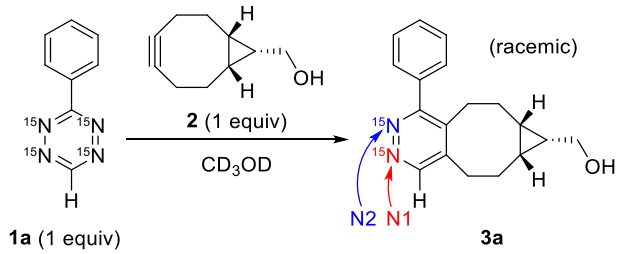

(1-Phenyl-6,6a,7,7a,8,9-hexahydro-5*H*-cyclopropa[5,6]cycloocta[1,2-*d*]pyridazin-7-yl-2,3-^{15}*N*$_2$)methanol (3a). To an NMR tube, was added a solution of **1a** (1.6 mg, 0.01 mmol, 1 equiv) in CD_3OD (200 µL), followed by a solution of (*1R,8S,9s*)-bicyclo[6.1.0]non-4-yn-9-ylmethanol **2** (1.5 mg, 0.01 mmol, 1 equiv) in CD_3OD (200 µL). The reaction was swirled for 15 seconds. Immediately upon addition, the color of the solution changed from pink (due to the pink color of the tetrazine **1a**) to colorless. NMR characterization spectra were obtained directly from this sample. The mixture was transferred to a vial and concentrated *in vacuo* to give **3a** as yellow oil (2.7 mg, 96%). Note that product appears to degrade on silica gel. **^{1}H NMR** (360 MHz, CD_3OD): **δ** 8.93–8.89 (dd, $J_{H\text{-}N1}$ = 10.4, $J_{H\text{-}N2}$ = 4.5 Hz, 1H), 7.55–7.53 (m, 3H), 7.48–7.45 (m, 2H), 3.71–3.61 (m, 2H), 3.19–3.11 (dt, *J* = 15.0, 5.9 Hz, 1H), 2.99–2.92 (m, 2H), 2.76–2.69 (dt, *J* = 14.4, 5.6 Hz, 1H), 2.38–2.29 (m, 1H), 2.13–2.05 (m, 1H), 1.74–1.58 (m, 2H), 1.15–1.06 (quint, *J* = 8.1 Hz, 1H), 1.02–0.88 (m, 2H); **^{15}N NMR** (36.5 MHz, CD_3OD): **δ** 372.8–371.2 (m, N1 and N2); **HRMS-LC/ESI** (m/z) Calc'd for ($C_{18}H_{21}{}^{15}N_2O^+$) ([M+H]$^+$): 283.1589; found: 283.1597.

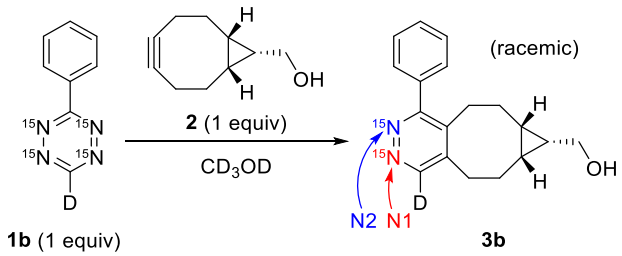

(1-Phenyl-6,6a,7,7a,8,9-hexahydro-5*H*-cyclopropa[5,6]cycloocta[1,2-*d*]pyridazin-7-yl-4-*d*-2,3-$^{15}N_2$)methanol (3b) Following the same procedure for **3a**, substituting **1b** for **1a**, **3b** was isolated as a yellow oil (2.8 mg, 100%). **^{1}H NMR** (360 MHz, CD_3OD): **δ** 7.54–7.53 (m, 3H), 7.47–7.45 (m, 2H), 3.71–3.61 (m, 2H), 3.19–3.11 (dt, *J* = 14.8, 5.9 Hz, 1H), 3.00–2.92 (m, 2H), 2.76–2.69 (dt, *J* = 14.0, 5.6 Hz, 1H), 2.38–2.30 (m, 1H), 2.13–2.04 (m, 1H), 1.74–1.58 (m, 2H), 1.15–1.06 (quint, *J* = 8.0 Hz, 1H), 1.03–0.87 (m, 2H); **^{15}N NMR** (36.5 MHz, CD_3OD): **δ** 372.6–371.3 (m, N1 and N2); **HRMS-LC/ESI** (m/z) Calc'd for ($C_{18}H_{20}D^{15}N_2O^+$) ($[M+H]^+$): 284.1652; found: 284.1657.

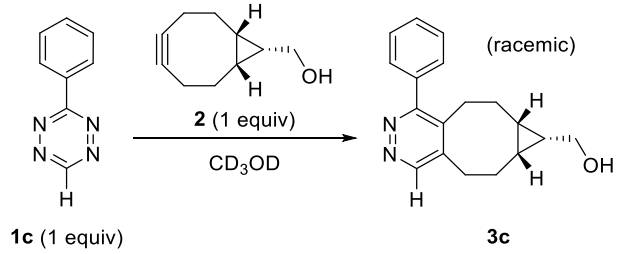

(1-Phenyl-6,6a,7,7a,8,9-hexahydro-5*H*-cyclopropa[5,6]cycloocta[1,2-*d*]pyridazin-7-yl)methanol (3c). To a 1-dram vial, was added a solution of **1c** (7.9 mg, 0.05 mmol, 1 equiv) in CD_3OD (3.33 mL) and a solution of **2** (7.5 mg, 0.05 mmol, 1 equiv) in CD_3OD (1.67 mL). Immediately upon addition, the color of the solution changed from pink (due to the pink color of the tetrazine **1c**) to colorless. After 15 seconds of shaking, the reaction mixture was concentrated *in vacuo* to give **3c** as a yellow oil (13.8 mg, 98%). Note that product appears to degrade on silica gel. **^{1}H NMR** (500 MHz, CD_3OD): **δ** 8.92 (s, 1H), 7.54-7.53 (m, 3H), 7.47-7.45 (m, 2H), 3.70-3.62 (m, 2H), 3.17–3.12 (dt, *J* = 14.3, 6.4 Hz, 1H), 2.98–2.92 (m, 2H), 2.75–2.70 (dt, *J* = 14.0, 5.5 Hz, 1H), 2.36–2.30 (m, 1H), 2.11–2.04 (m, 1H), 1.72–1.59 (m, 2H), 1.13–1.07 (quint, *J* = 8.2 Hz, 1H), 1.01–0.90 (m, 2H); **^{13}C NMR** (125 MHz, CD_3OD): **δ** 163.6, 153.1, 145.3, 142.9, 138.5, 130.1, 129.5, 59.3, 31.4, 28.5, 24.7, 22.9, 20.4, 19.9; **FTIR** (thin film, CH_2Cl_2): 3320 (br), 2921, 1679 (br), 1558, 1445, 1350, 1020, 763, 731, 700 cm^{-1}; **HRMS-LC/ESI** (m/z) Calc'd for ($C_{18}H_{21}N_2O^+$) ($[M+H]^+$): 281.1648; found: 281.1654.

1.4. Kinetic Characterization of Tetrazine/Cyclooctyne Reaction

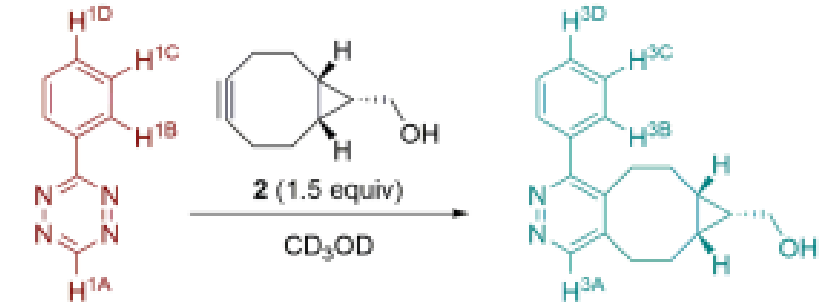

1c (1 equiv) **3c**

Emulating hyperpolarization conditions (see §2.1), a 1.5 mM solution of **1c** (1 equiv) in CD_3OD (400 µL) was added to an NMR tube. To this solution, a 4.5 mM solution of **2** (1.5 equiv) in CD_3OD (200 µL) was added and the NMR tube was shaken vigorously. Immediately upon addition, the color of the solution changed from pink (due to the pink color of the tetrazine **1c**) to colorless. As soon as the pink color completely dissipated (<2 seconds), the sample was placed into the NMR and a spectrum was acquired. Spectral comparisons are shown in **fig. S1** below. The spectra after reaction corresponds with the spectra for **3c** (see §1.3 and respective spectra in §3).

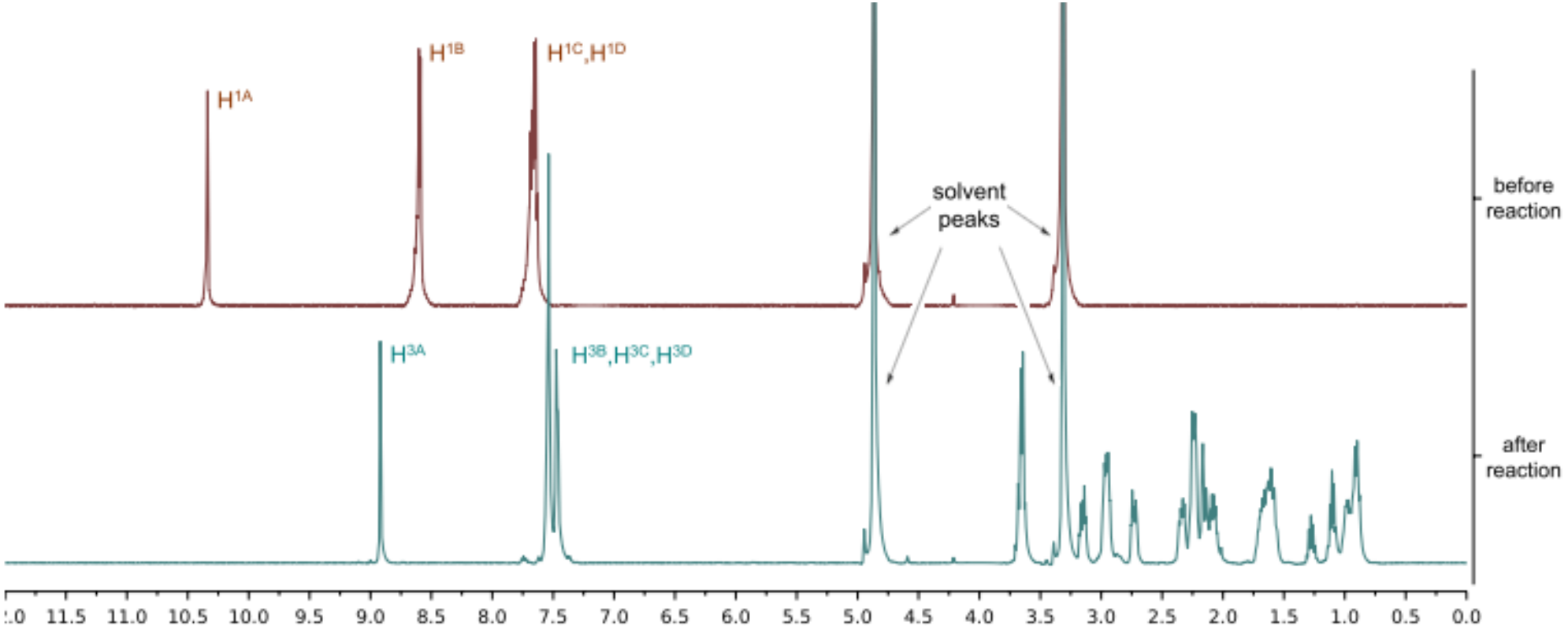

. **fig. S1. ^{1}H NMR comparison between tetrazine and cycloaddition product.**

2. Hyperpolarization experiments

2.1. Hyperpolarization Protocols

Hyperpolarization Setup. A high-pressure gas delivery system was specially built for the SABRE-SHEATH process. Normal H_2 gas is converted to *para*-H_2 (enrichment ~90.2%) using a commercial *para*-H_2 generator. The *para*-H_2 gas is delivered to the sample solution through a capillary at a pressure of about 100 psi. The magnetically shielded environment was prepared using a 3-layer μ-metal magnetic shield. A solenoid placed inside the shield controls the magnetic field via manual adjustment of the voltage using a DC voltage output and a resistor. A separate capillary for the injection of a secondary solution was added adjacent to the *para*-H_2 delivery line, with a valve placed at the site of injection to seal the pressure when bubbling gas, as shown in **fig. S2**.

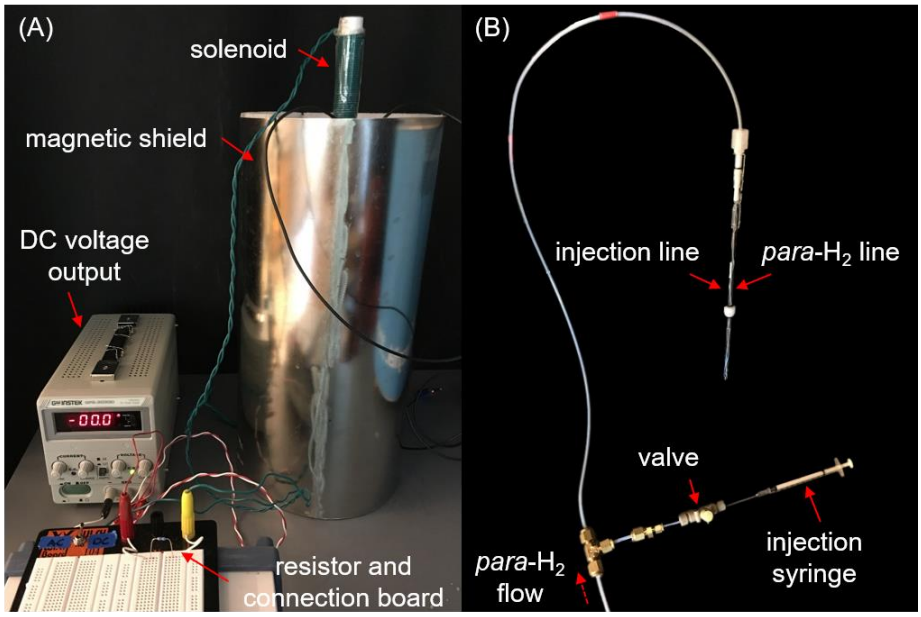

fig. S2. Experimental setup for hyperpolarization and hyperpolarized reaction experiments. a, The device used to hyperpolarize the tetrazine precursors, composed of: a DC voltage output, a magnetic shield, a solenoid, and a resistor. **b,** The sample tube and the injection line, together with the *para*-H_2 flow line.

Sample Preparation. Unless otherwise described, a solution of ^{15}N-enriched tetrazine (**1a** or **1b,** 1.5 mM), pyridine (1.0 mM), and Ir(IMes)(COD) Cl (0.15 mM) in methanol-d_4 (400 µL) was prepared.(*43*) Note: IMes = 1,3-bis(2,4,6-trimethylphenyl) imidazol-2-ylidene; COD = 1,5-cyclooctadiene.

Tetrazine Hyperpolarization Procedure. The Ir catalyst was pre-activated by bubbling *para*-H_2 through a solution of tetrazine, pyridine, and Ir catalyst (sample preparation described above) for 30 minutes. Following pre-activation, the tetrazine was hyperpolarized, either magnetization or singlet order.

- To hyperpolarize magnetization, the solution was placed inside the magnetic shield, with the magnetic field adjusted to 0.4 µT (using a solenoid of 430 mm with 205 turns and a voltage of 7.5 V across 11.4 kOhms). After 3 minutes' bubbling of *para*-H_2, the gas flow was stopped and the sample was manually transferred from the low field to an 8.5 T spectrometer for signal read out as quickly as possible. This manual transfer takes ~8 seconds, and a 90˚ pulse-acquire sequence was used for read out.

- To hyperpolarize singlet, the sample was placed at a magnetic field of 0.3 mT and *para*-H_2 was bubbled through the solution for 3 minutes. As described in the above procedure, the sample was then manually transferred to an 8.5 T spectrometer as quickly as possible and detected using a 90˚ pulse-acquire sequence.

Tetrazine Hyperpolarization and Cycloaddition Reaction Procedure. For the hyperpolarization of the cycloaddition products **3a** and **3b**, a solution of tetrazine (**1a** or **1b**, respectively), pyridine, and Ir catalyst in methanol-d_4 was first hyperpolarized at 0.4 µT or 0.3 mT, depending on which spin order was studied (solution preparation and hyperpolarization procedure described above). After hyperpolarization, the *para*-H_2 gas flow was stopped and the pressure was released through the exhaust outlet, after which the injection valve (shown in **fig. S2**) was quickly opened to inject a solution of cyclooctyne **2** (4.5 mM) in methanol-d_4 (200 µL) (equiv of tetrazine : **2** = 1.0 : 1.5). Injection was completed in less than 1 second, and the sample was shaken for 3 seconds to reach complete reaction, visually evidenced by the color change from pink (i.e., the color of the tetrazine) to transparent. The sample was then manually transferred to an 8.5 T spectrometer for product signal read out.

2.2. Concentration Dependence of Tetrazine Hyperpolarization

The influence of solution concentration on the enhancement and lifetime of both tetrazine magnetization and singlet hyperpolarization was studied.

Using serial dilution, solutions of tetrazine **1a**, pyridine, and Ir catalyst in methanol-d_4 (400 µL) were prepared at different concentrations, but in the same ratio of each component:

- **1a** (7.5 mM), pyridine (5.0 mM), and Ir(IMES)(COD)Cl (0.75 mM)
- **1a** (3.8 mM), pyridine (2.5 mM), and Ir(IMES)(COD)Cl (0.38 mM)
- **1a** (1.5 mM), pyridine (1.0 mM), and Ir(IMES)(COD)Cl (0.15 mM) (i.e., default concentrations of solution used in all other experiments)
- **1a** (0.60 mM), pyridine (0.40 mM), and Ir(IMES)(COD)Cl (0.060 mM)

For the rest of this section, samples are referred to by the concentration of tetrazine **1a** comprising the solution. As described in §2.1, either magnetization or singlet tetrazine hyperpolarization was developed following pre-activation of the catalyst. After bubbling *para*-H_2 through the sample, the sample was transferred to 0.3 mT for a variable period of time. Following this delay, the sample was transported to the magnet and the spectrum was immediately recorded with a 90° pulse-acquire sequence. Triplet magnetization signal was deconvoluted from singlet signal, and fitted to a single exponential decay. Data are given in **table S1** and displayed in **fig. S3**.

table S1. Magnetization and singlet enhancements and lifetimes at variable concentrations. (Note that 1.5 mM tetrazine is the concentration used in all other experiments described.)

Tetrazine (**1a**) Concentration (mM)	Z-Magnetization enhancement at 0s delay (normalized to 1.5 mM Z-magnetization, %)	T_1 (s)	Singlet enhancement at 0s delay (normalized to 1.5 mM singlet, %)	T_s (s)
7.5	66	47	56	48
3.75	86	72	77	58
1.5	100	91	100	137
0.60	130	74	96	357

Note that when concentration of the tetrazine was lowered to 0.40 mM (and concentrations of other components were decreased proportionally), the enhancement dropped sharply for both magnetization and singlet (data not shown), and, due to low signal-to-noise ratio, lifetimes were not able to be calculated.

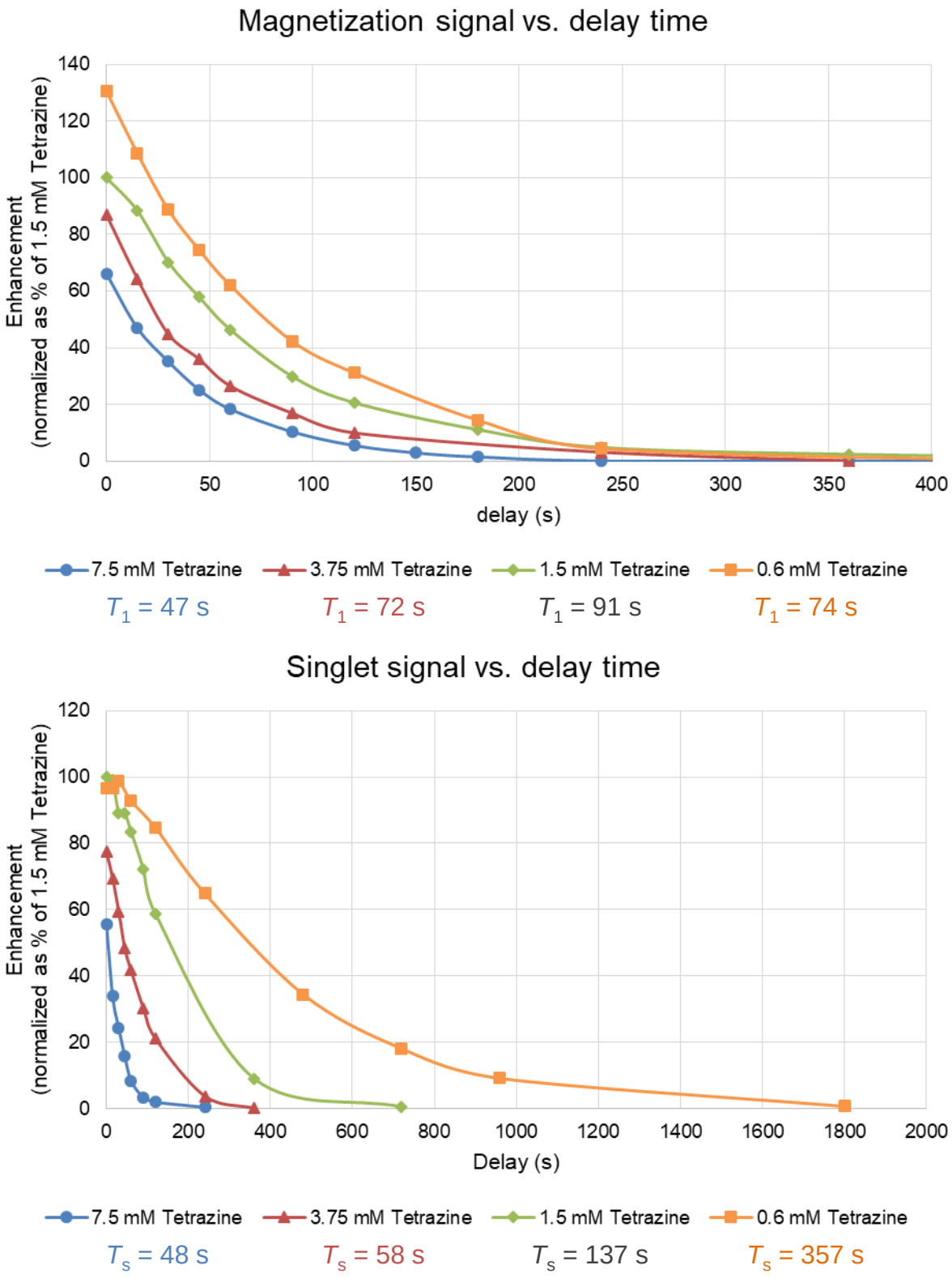

fig. S3. Hyperpolarized signal decay of magnetization and singlet at variable concentrations. Lifetimes and enhancements for each concentration summarized in **table S1.**

2.3. Magnetic Field Dependence of Tetrazine Hyperpolarization

The magnetic field dependence of hyperpolarization was studied in the following set of experiments. We found that the magnetization only polarizes in the low-field environment that is created inside the shield, and that there is a sharp drop in magnetization hyperpolarization at higher fields. From the magnified inset in **fig. S4**, we can see that the magnetization polarization reaches its maximum at a magnetic field of ~0.3 μT.

In contrast, the singlet spin order is hyperpolarized in a very broad range of magnetic fields, from 0.2 mT to 100 mT. Bubbling the sample at ~3 mT yields the best signal; however, for experimental convenience, we chose to use 0.3 mT as our standard magnetic field for singlet hyperpolarization, which gives similar signal strength to that at 3 mT. The field dependence results are summarized in **fig. S4**.

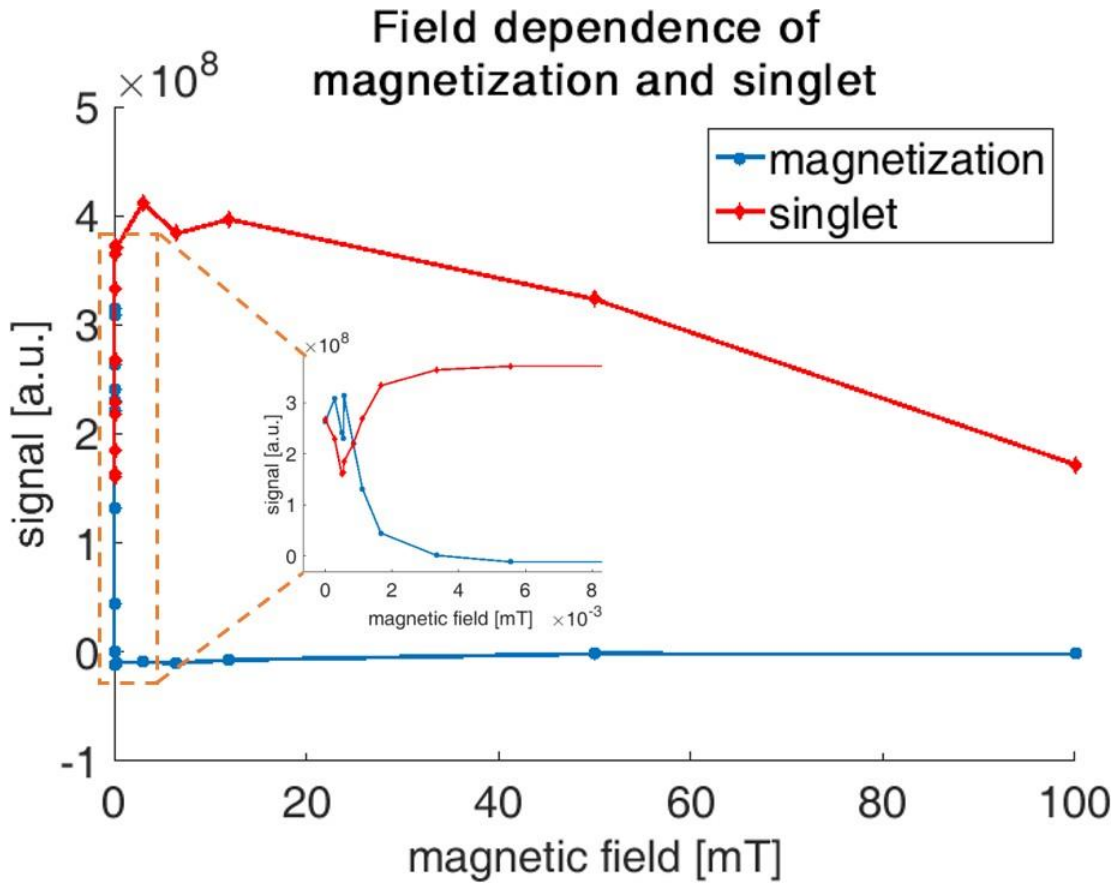

fig. S4. Hyperpolarization of magnetization and singlet as a function of magnetic field. The magnetization can only be hyperpolarized at very low magnetic fields, while the singlet has a much broader resonance condition. Magnified inset: in the low-field region, we can see that the magnetization and singlet spin order has opposite polarization patterns: when one increases, the other decreases. Though the singlet has broad resonance condition, the optimal field is ~3 mT, and as the strength of the magnetic field is increased to very high values, the polarization level drops significantly.

2.4. Dilution Effect on Hyperpolarization

To observe the effect of simple dilution on hyperpolarization, pure methanol-d_4 was injected into a solution of hyperpolarized tetrazine to obtain a diluted hyperpolarized signal as follows: tetrazine **1a** was hyperpolarized singlet order at 0.3 mT and the spectra were acquired (as described in §2.1). The sample was again bubbled with *para*-H_2 for 3 minutes at 0.3 mT, then the pressure was released and the injection valve was opened, after which 200 µL of methanol-d_4 was quickly injected and the sample was manually transferred into the magnet to read out the signal (detailed in §2.1, but with the key difference: pure methanol-d_4 used instead of a solution of **2** in methanol-d_4). The signal following dilution of the solution, overlapped with the signal before dilution, is shown in **fig. S5**. Based on this dilution test, we can confirm that addition of methanol does not alter the hyperpolarized precursor, but it does quench the signal slightly. The signal observed was about half of the signal before addition.

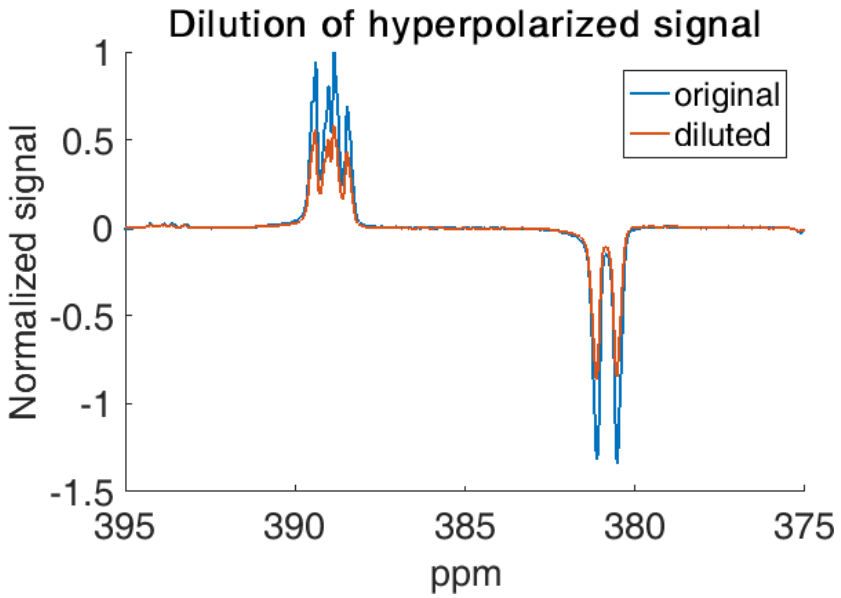

fig. S5. Comparison of the originally hyperpolarized singlet and diluted signal. Injection of 200 µL methanol-d_4 will not alter the signal, but will decrease its intensity by about two-fold. We chose to perform this test using the hyperpolarized singlet because the injection will introduce an additional ~3 seconds delay (due to release of *para*-H_2 pressure and injection of methanol), which may have a larger effect for magnetization due to its short relaxation time.

2.5. Injection and Detection with Small Tip Angle

In addition to using a 90˚ pulse-acquire sequence for detection after injection, we performed experiments using small tip angles (15˚ or 11.25˚) to acquire a series of detection within a short time window (~ 10 s), from which we can determine the relaxation lifetime of different spin orders of the hyperpolarized product. The results are shown in **fig. S6**.

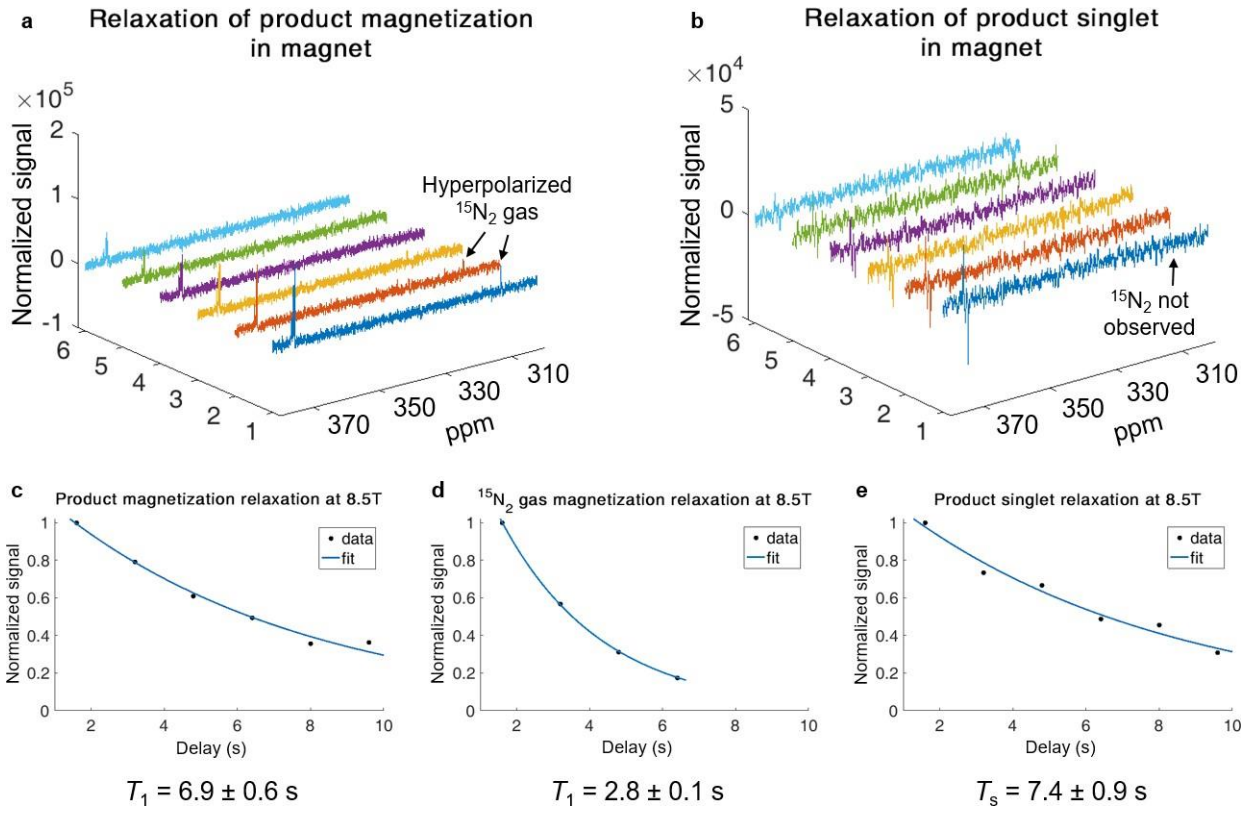

fig. S6. Small-tip-angle spectra of the hyperpolarized cycloaddition product 3a. a, Magnetization of ^{15}N-enriched tetrazine **1a** is first hyperpolarized at 0.4 μT, then a solution of **2** in methanol-d_4 is injected (as described in §2.1). Then, the sample is manually transferred as quickly as possible into the magnet, using 15˚ tip angle to acquire 6 spectra consecutively, with a 1.6 s delay between each acquisition. The product shows in-phase signal at ~372 ppm, and at ~310 ppm, we can clearly see a singlet corresponding to hyperpolarized $^{15}N_2$ gas in the first 4 spectra. **b,** Singlet spin order of ^{15}N-enriched tetrazine **1a** is first hyperpolarized at 0.3 mT, then a solution of **2** in methanol-d_4 is injected (as described in §2.1). Then, the sample is manually transferred as quickly as possible into the magnet, using 11.25˚ tip angle to acquire 6 spectra consecutively, with a 1.6 s delay between each acquisition. As expected, the product shows anti-phase signal at ~372 ppm, but at ~310 ppm there is no signal, indicating that *para*-N_2 is generated (thus yielding no ^{15}N signal). **c-e,** Relaxation constant measurements of the hyperpolarized product magnetization, hyperpolarized $^{15}N_2$ gas, and hyperpolarized product singlet. The product magnetization has T_1 lifetime of ~6.9 s, which is quite similar as T_s (~7.4 s), and this is consistent with the 90˚ pulse acquisition measurements detailed in the main manuscript.

2.6. Hyperpolarization in Aqueous Media

One important aspect of our bioorthogonal reaction-promoted hyperpolarization approach is the ability to exploit this scheme using an aqueous solvent, which is critical for many biological reactions and would widely broaden the applicability of this strategy. We attempted to use D_2O as a solvent at higher temperatures for tetrazine hyperpolarization; however, the substrates did not hyperpolarize. We achieved our best results using a 3:1 methanol-d_4:D_2O mixture and by elevating the temperature to about 50˚C using a water bath while bubbling *para*-H_2 through the solution. As shown in **fig. S7, a**, the tetrazine precursor **1a** hyperpolarized with an enhancement of ~900 (p = 0.27%), about 30% compared to that in neat methanol-d_4.

A solution of **2** was prepared in the same 3:1 methanol-d_4:D_2O mixed solvent and was injected after the hyperpolarization was established for the precursor tetrazine. As expected, though we could still observe the hyperpolarized product signal, the polarization level was much lower than previous experiments (**fig. S7, b)**, and this could be due to several reasons, one of which is viscosity. The viscosity of the water-containing solvent is much higher, and thus causes numerous problems: the *para*-H_2 does not flow as smoothly, the hyperpolarization may relax faster, and it will be more difficult for the injected compound to react well with the precursor (e.g., residual tetrazine peaks were still observed after injection; it was difficult to homogenize the sample by shaking, since the surface tension of the water limited movement of the liquid in the NMR tube). More efforts need to be put in the improvements of solvent for broader and better applications for SABRE-SHEATH to be used in biologically or biochemically related reactions.

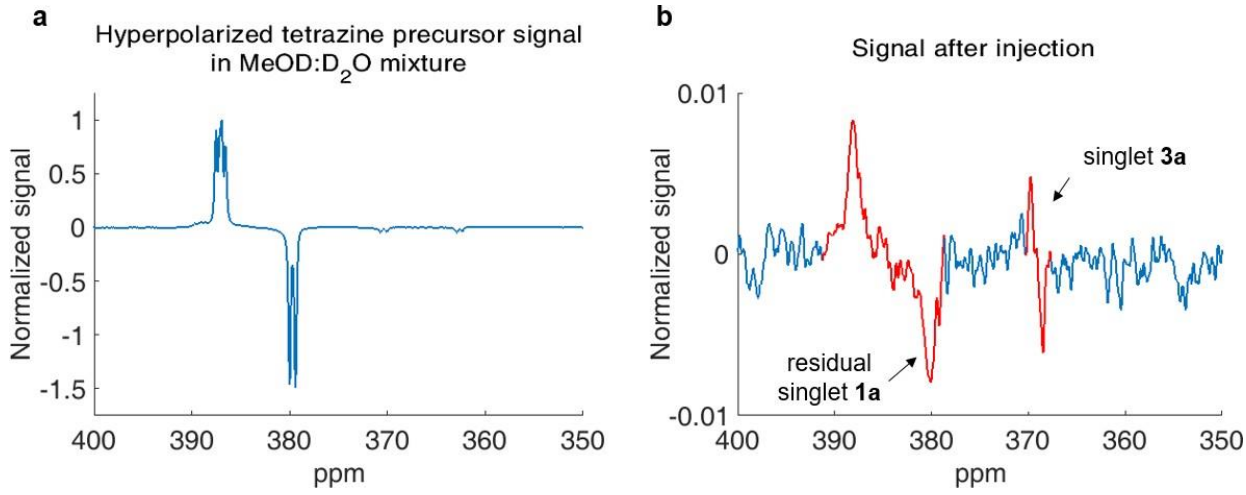

fig. S7. SABRE-SHEATH experiment using methanol-d_4/D_2O mixture as solvent. a, The ^{15}N-tetrazine precursor can be hyperpolarized using the same protocol as described in §2.1. However, the signal after injection is quite small: only ~1% of the hyperpolarized signal is observed as shown in **b**, and there is large amount of residual tetrazine left, which could be caused by the high viscosity of the solvent; thus, the compound cannot completely react in a short time period of 3 seconds.

3. ^{1}H, ^{13}C, and ^{15}N spectra

- ^{1}H, ^{13}C, and ^{15}N spectra of **1a**
- ^{1}H, ^{13}C, and ^{15}N spectra of **1b**
- ^{1}H and ^{13}C spectra of **1c**
- ^{1}H and ^{15}N spectra of **3a**
- ^{1}H and ^{15}N spectra of **3b**
- ^{1}H and ^{13}C spectra of **3c**
- ^{15}N spectra of $^{15}N_2$

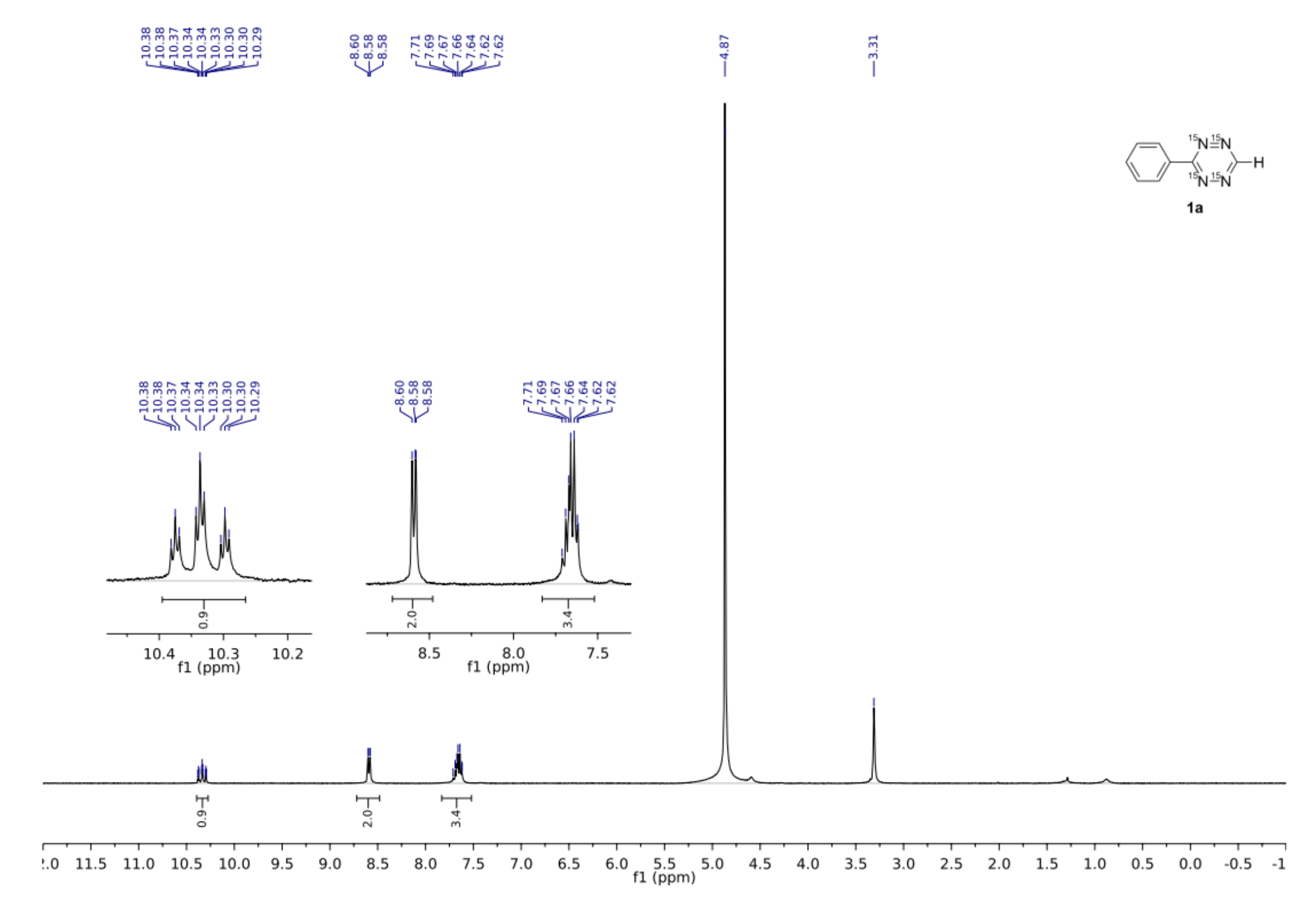
10.38
10.38
10.37
10.34
10.34
10.33
10.30
10.30
10.29
8.60
8.58
8.58
7.71
7.69
7.67
7.66
7.64
7.62
7.62
4.87
3.31
15N
15N
H
15N
15N
1a
0.9
2.0
3.4
f1 (ppm)

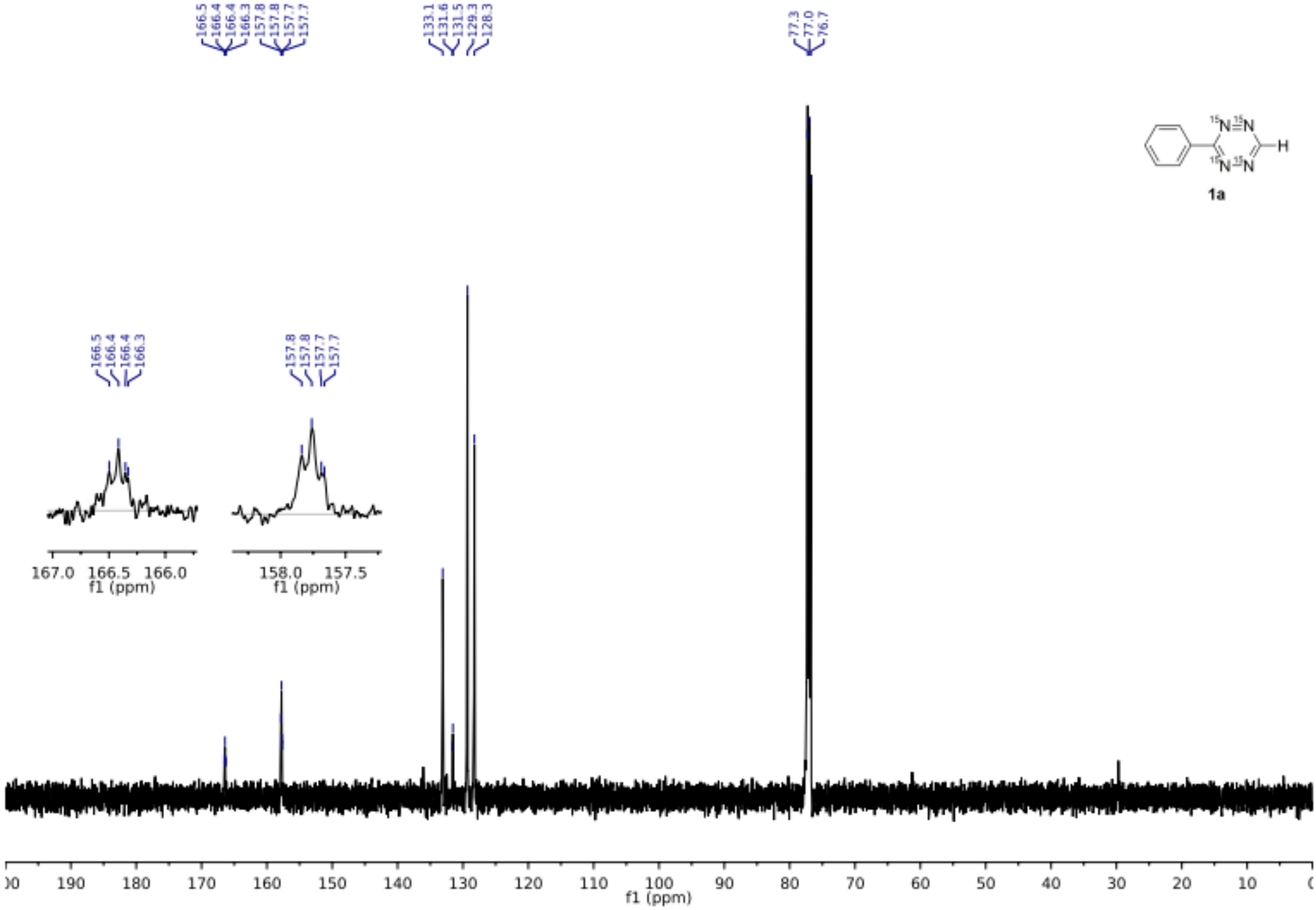
166.5
166.4
166.4
166.3
157.8
157.8
157.7
157.7
133.1
131.6
131.5
129.3
128.3
77.3
77.0
76.7
166.5
166.4
166.4
166.3
157.8
157.8
157.7
157.7
167.0 166.5 166.0
f1 (ppm)
158.0 157.5
f1 (ppm)
H
1a
f1 (ppm)

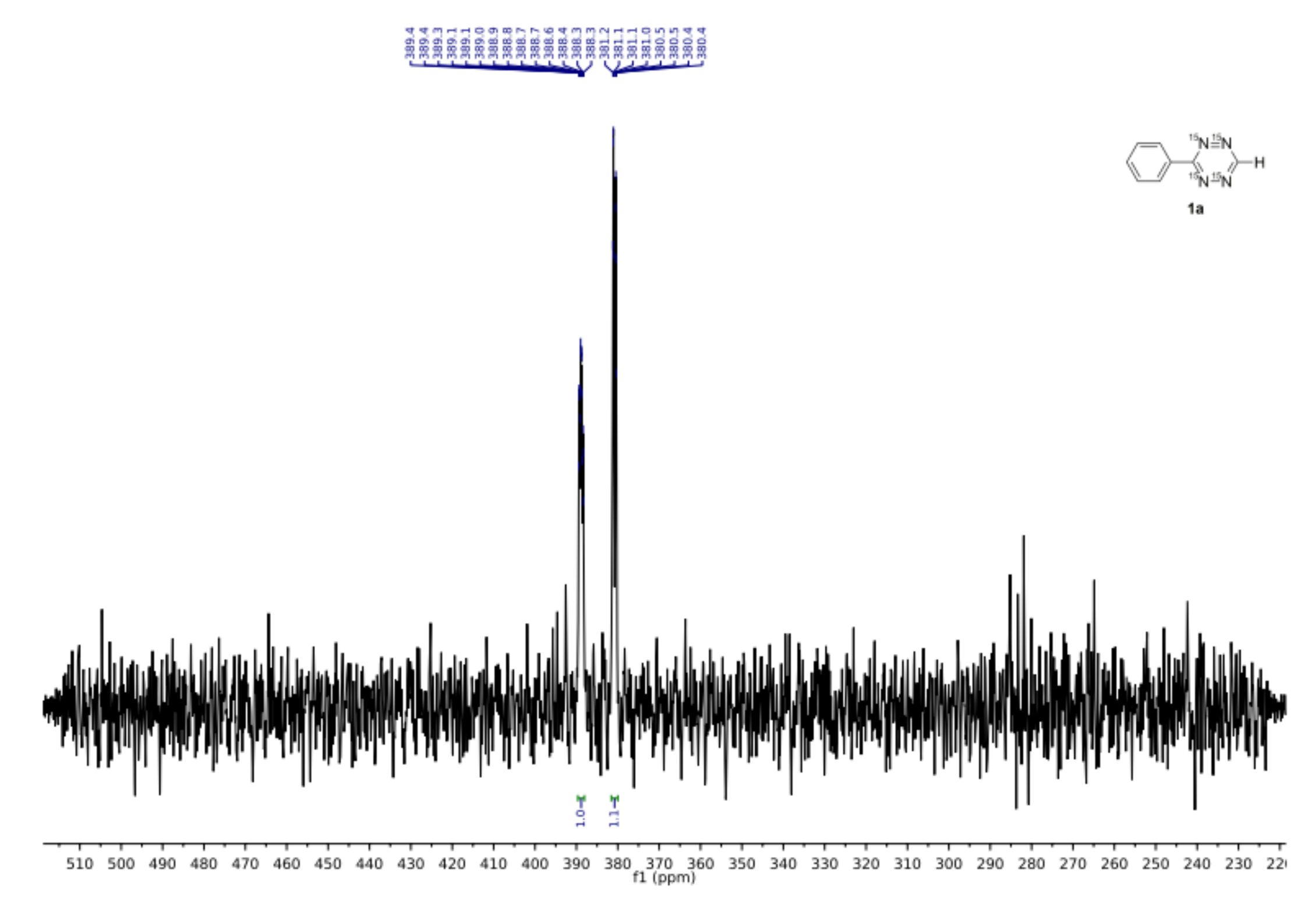
389.4
389.4
389.3
389.1
389.1
389.0
388.9
388.8
388.7
388.7
388.6
388.4
388.3
388.3
381.2
381.1
381.1
381.0
380.5
380.5
380.4
380.4
^{15}N
^{15}N
H
^{15}N
^{15}N
1a
1.0
1.1
510 500 490 480 470 460 450 440 430 420 410 400 390 380 370 360 350 340 330 320 310 300 290 280 270 260 250 240 230
f1 (ppm)

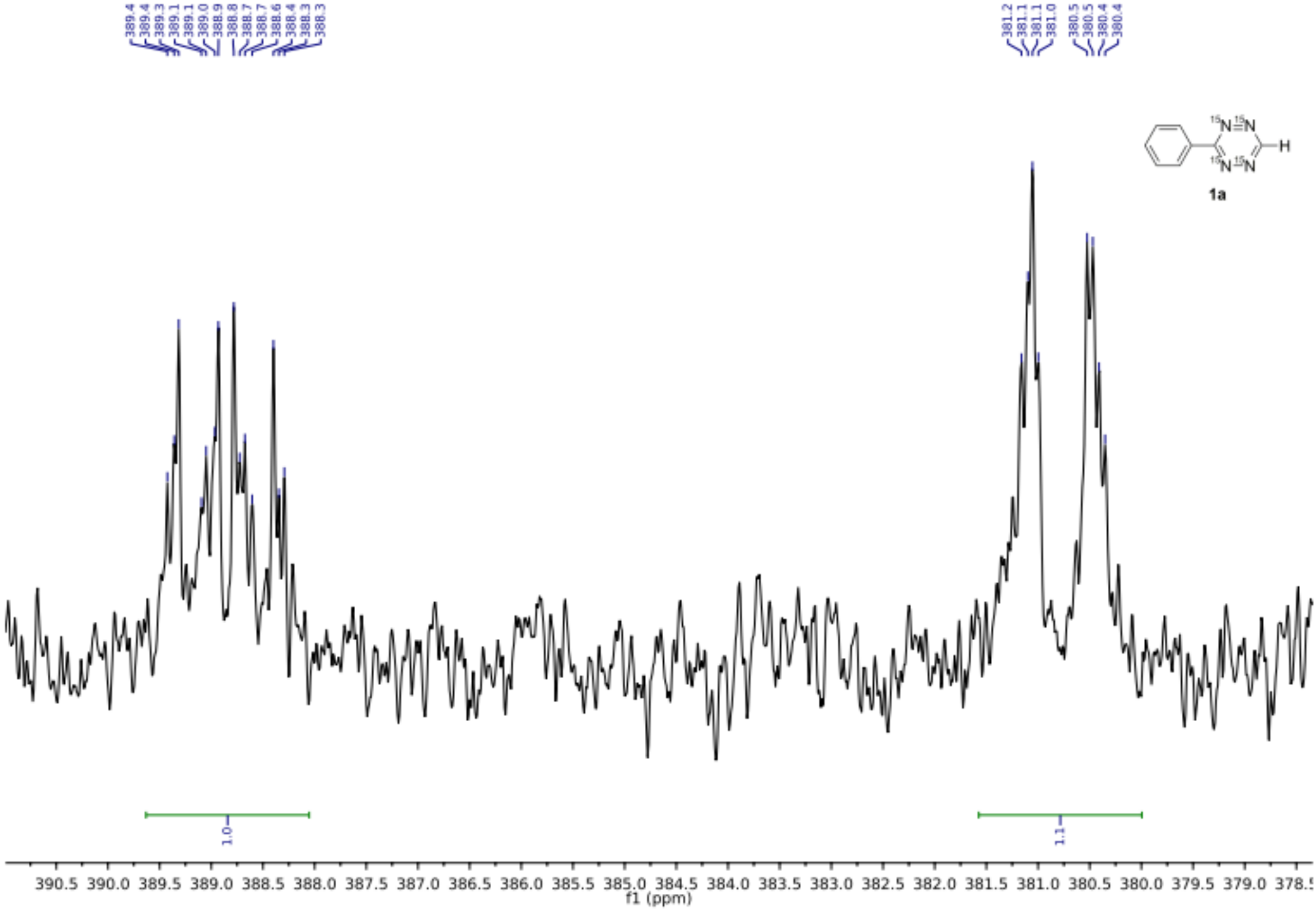
389.4
389.4
389.3
389.1
389.1
389.0
388.9
388.8
388.7
388.7
388.6
388.4
388.3
388.3
381.2
381.1
381.1
381.0
380.5
380.5
380.4
380.4
15N
15N
H
15N
15N
1a
1.0
1.1
390.5 390.0 389.5 389.0 388.5 388.0 387.5 387.0 386.5 386.0 385.5 385.0 384.5 384.0 383.5 383.0 382.5 382.0 381.5 381.0 380.5 380.0 379.5 379.0 378.5
f1 (ppm)

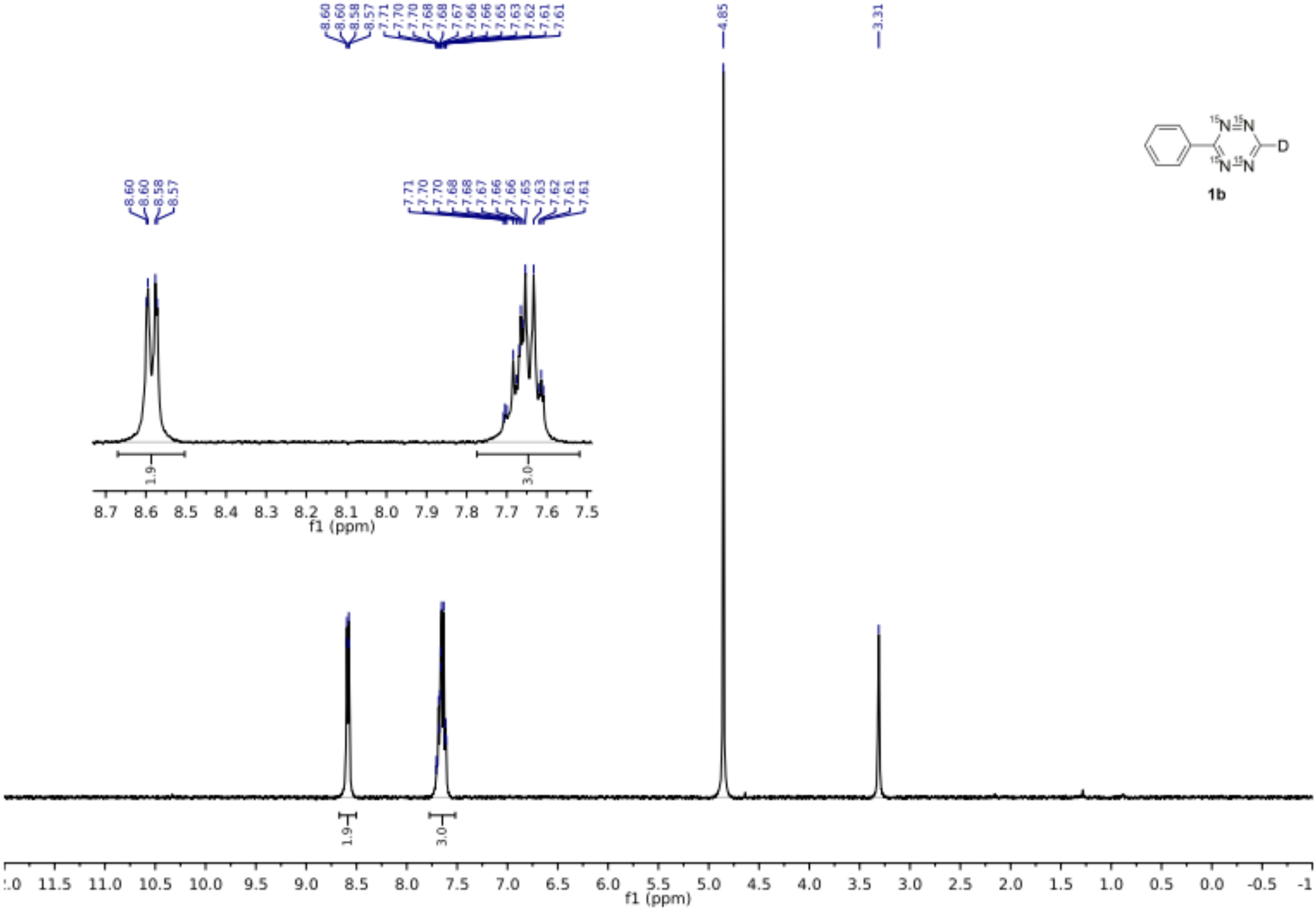
8.60
8.60
8.58
8.57
7.71
7.70
7.70
7.68
7.68
7.67
7.66
7.66
7.65
7.63
7.62
7.61
7.61
4.85
3.31
1.9
3.0
8.7 8.6 8.5 8.4 8.3 8.2 8.1 8.0 7.9 7.8 7.7 7.6 7.5
f1 (ppm)
15N
15N
15N
15N
D
1b
1.9
3.0
:.0 11.5 11.0 10.5 10.0 9.5 9.0 8.5 8.0 7.5 7.0 6.5 6.0 5.5 5.0 4.5 4.0 3.5 3.0 2.5 2.0 1.5 1.0 0.5 0.0 -0.5 -1
f1 (ppm)

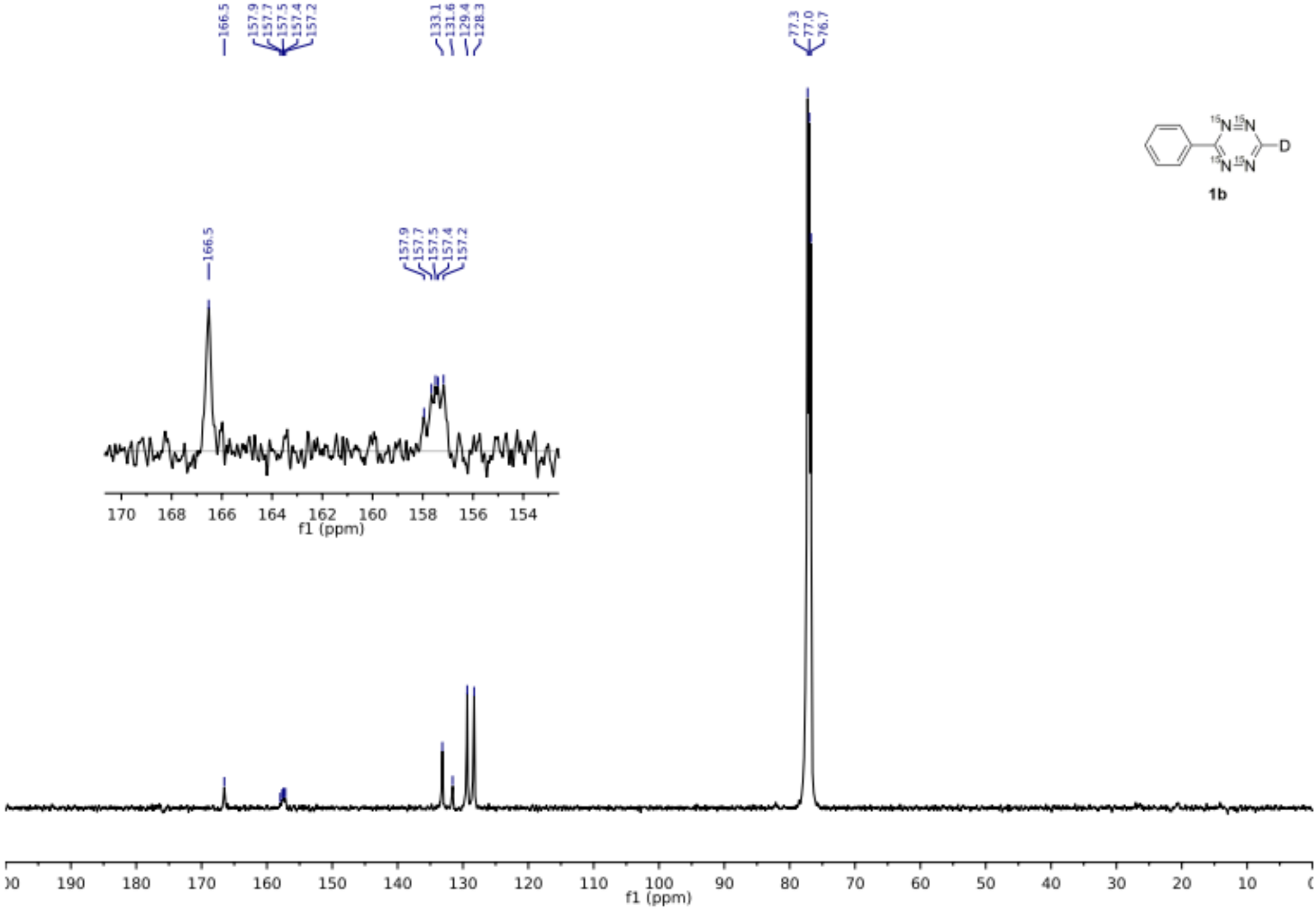
166.5
157.9
157.7
157.5
157.4
157.2
133.1
131.6
129.4
128.3
77.3
77.0
76.7
166.5
157.9
157.7
157.5
157.4
157.2
170 168 166 164 162 160 158 156 154
f1 (ppm)
190 180 170 160 150 140 130 120 110 100 90 80 70 60 50 40 30 20 10
f1 (ppm)
D
1b

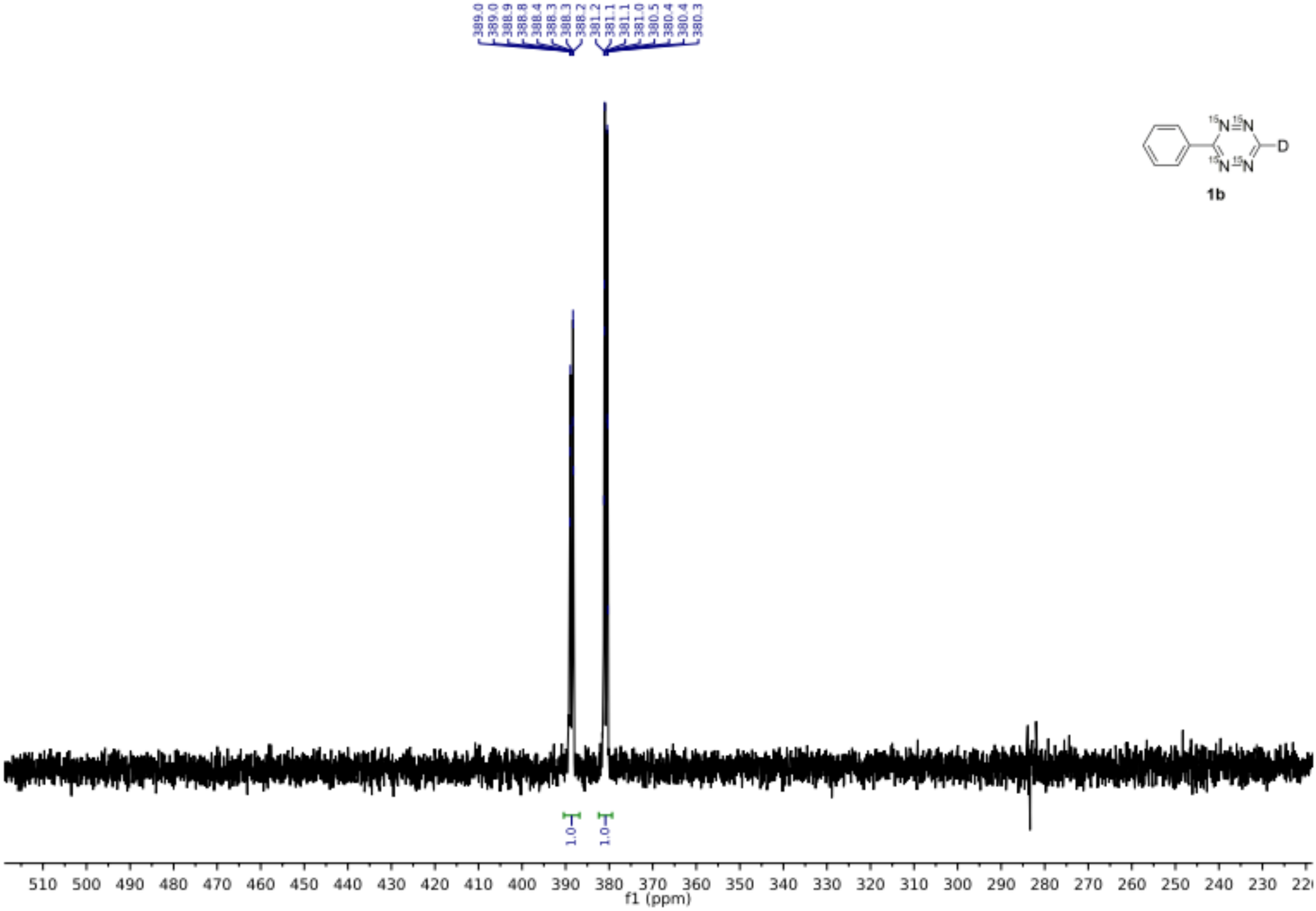
389.0
389.0
388.9
388.8
388.4
388.3
388.3
388.2
381.2
381.1
381.1
381.0
380.5
380.4
380.4
380.3
1.0
1.0
510 500 490 480 470 460 450 440 430 420 410 400 390 380 370 360 350 340 330 320 310 300 290 280 270 260 250 240 230
f1 (ppm)

15N
15N
D
15N
15N

1b

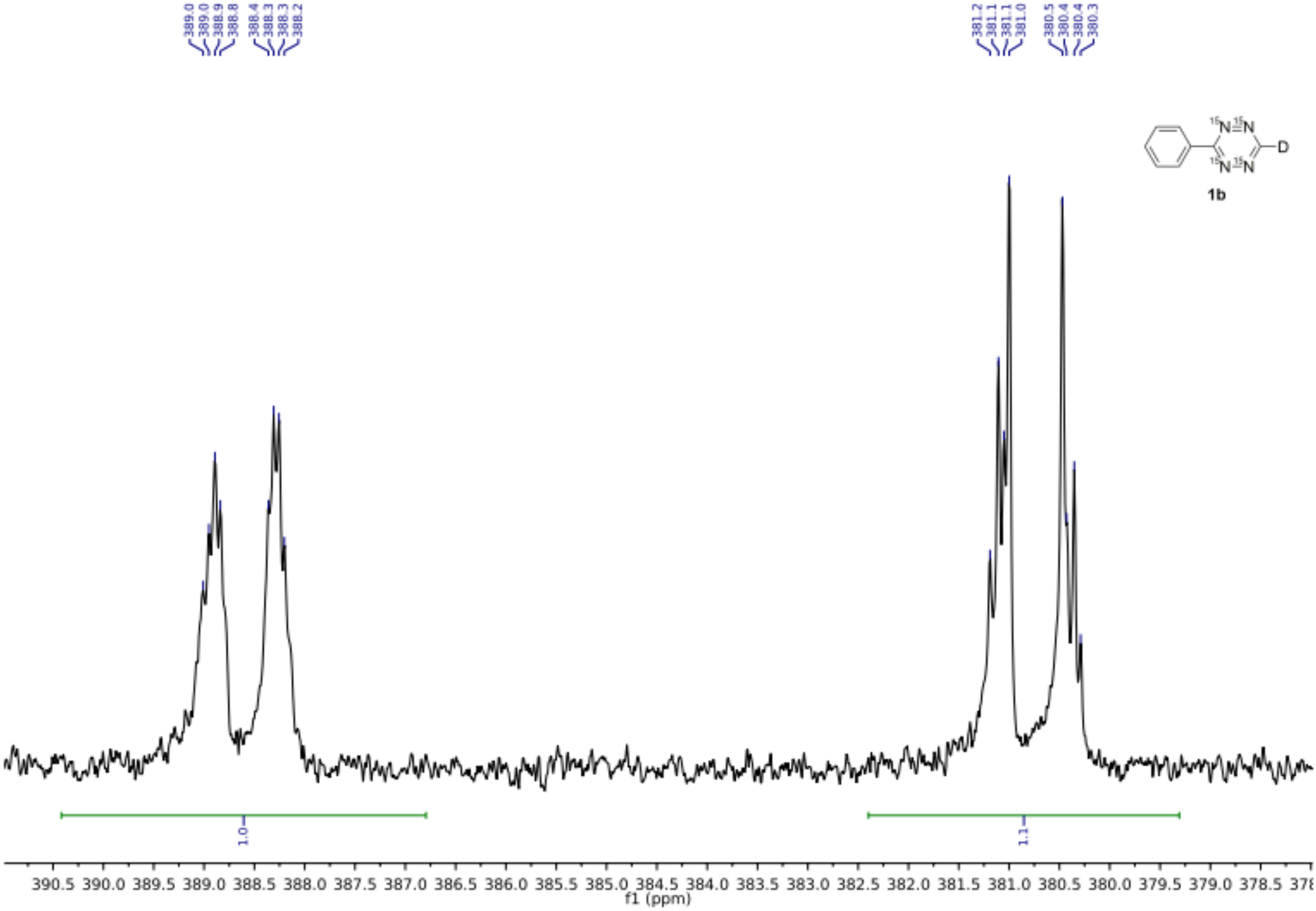
389.0
389.0
388.9
388.8
388.4
388.3
388.3
388.2
381.2
381.1
381.1
381.0
380.5
380.4
380.4
380.3
1b
1.0
1.1
390.5 390.0 389.5 389.0 388.5 388.0 387.5 387.0 386.5 386.0 385.5 385.0 384.5 384.0 383.5 383.0 382.5 382.0 381.5 381.0 380.5 380.0 379.5 379.0 378.5
f1 (ppm)

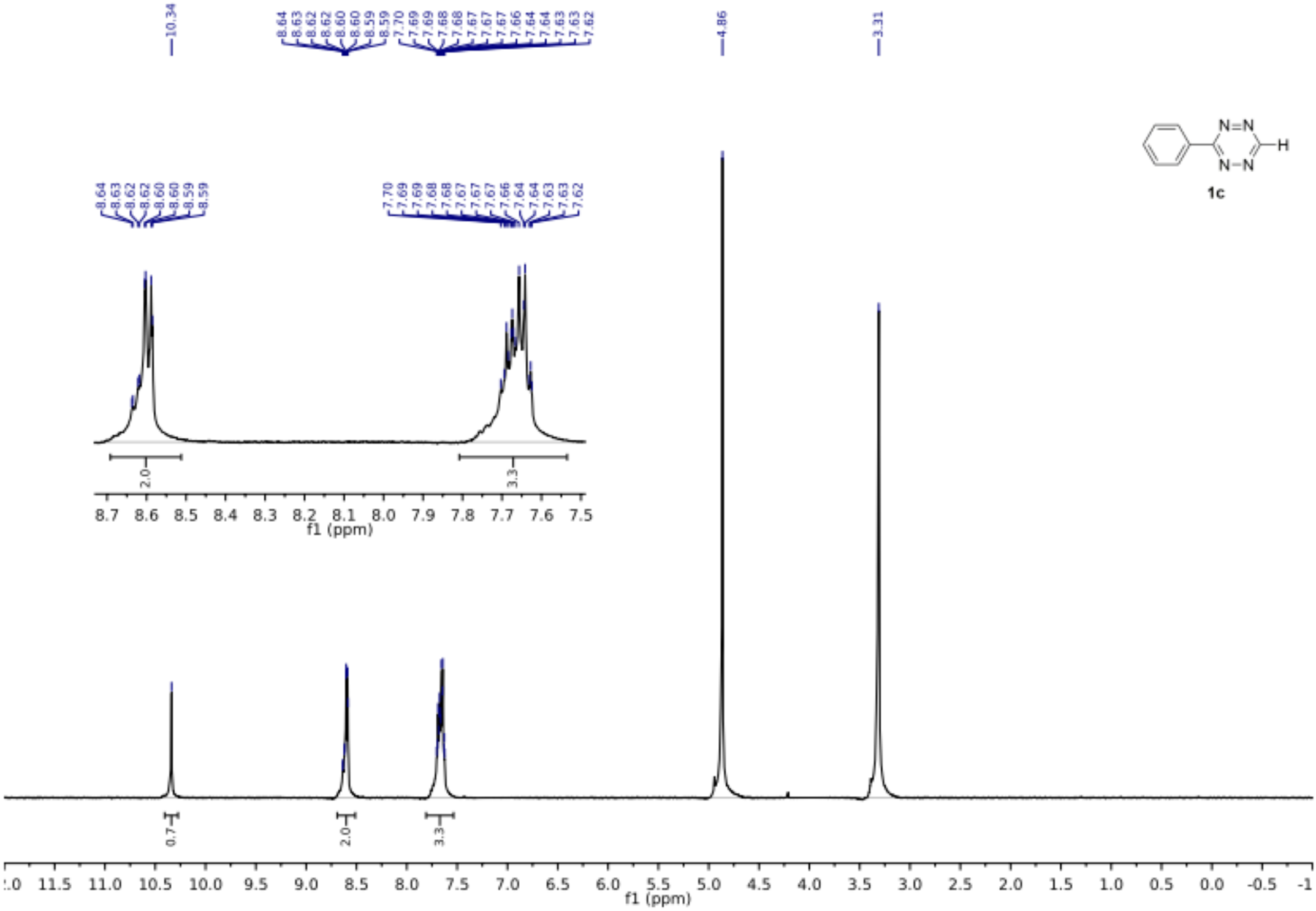
10.34
8.64
8.63
8.62
8.62
8.60
8.60
8.59
8.59
7.70
7.69
7.69
7.68
7.68
7.67
7.67
7.67
7.66
7.64
7.64
7.63
7.63
7.62
4.86
3.31
N=N
N-N
H
1c
2.0
3.3
8.7 8.6 8.5 8.4 8.3 8.2 8.1 8.0 7.9 7.8 7.7 7.6 7.5
f1 (ppm)
0.7
2.0
3.3
:.0 11.5 11.0 10.5 10.0 9.5 9.0 8.5 8.0 7.5 7.0 6.5 6.0 5.5 5.0 4.5 4.0 3.5 3.0 2.5 2.0 1.5 1.0 0.5 0.0 -0.5 -1
f1 (ppm)

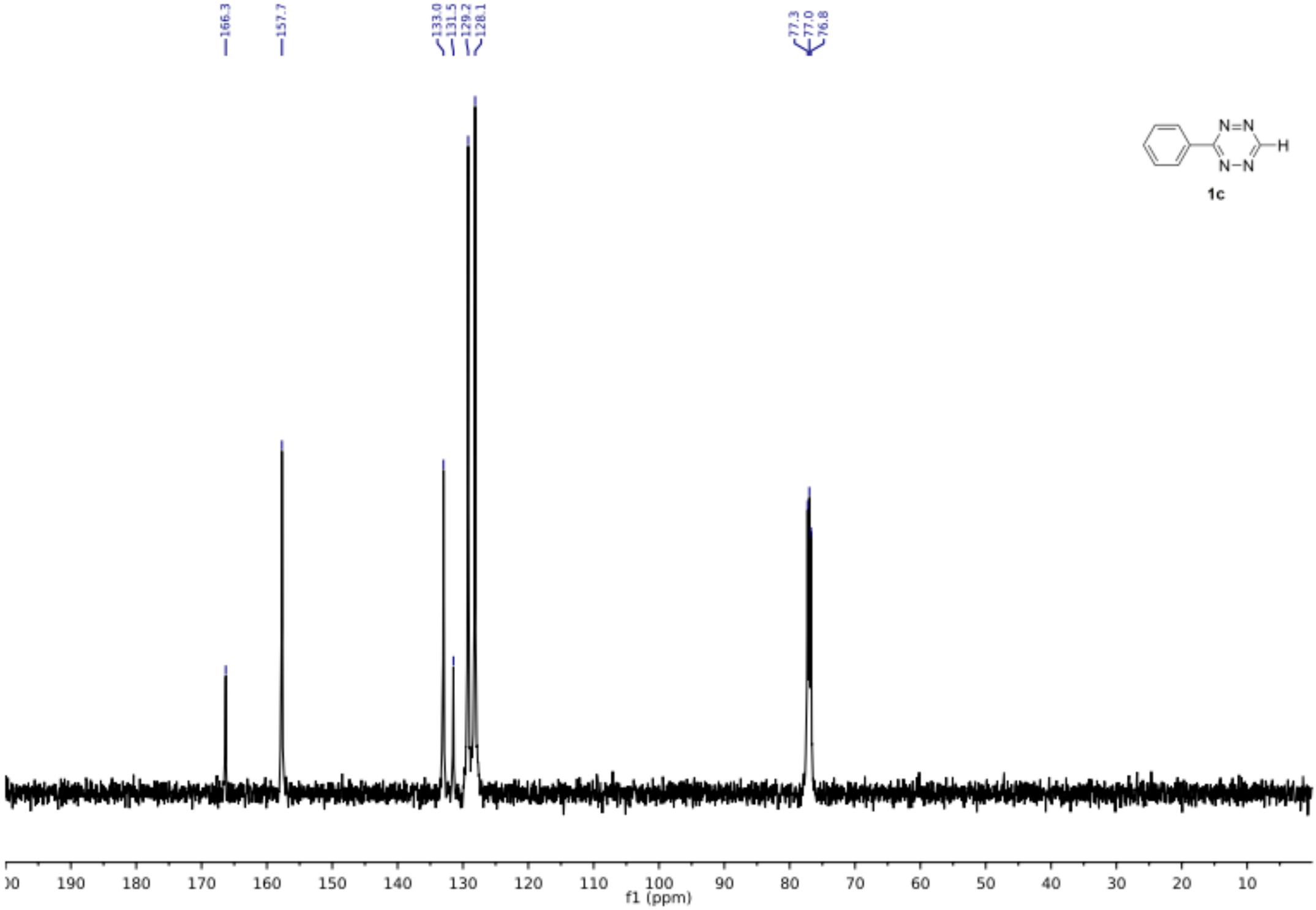
166.3
157.7
133.0
131.5
129.2
128.1
77.3
77.0
76.8
N=N
N–N
H
1c
f1 (ppm)

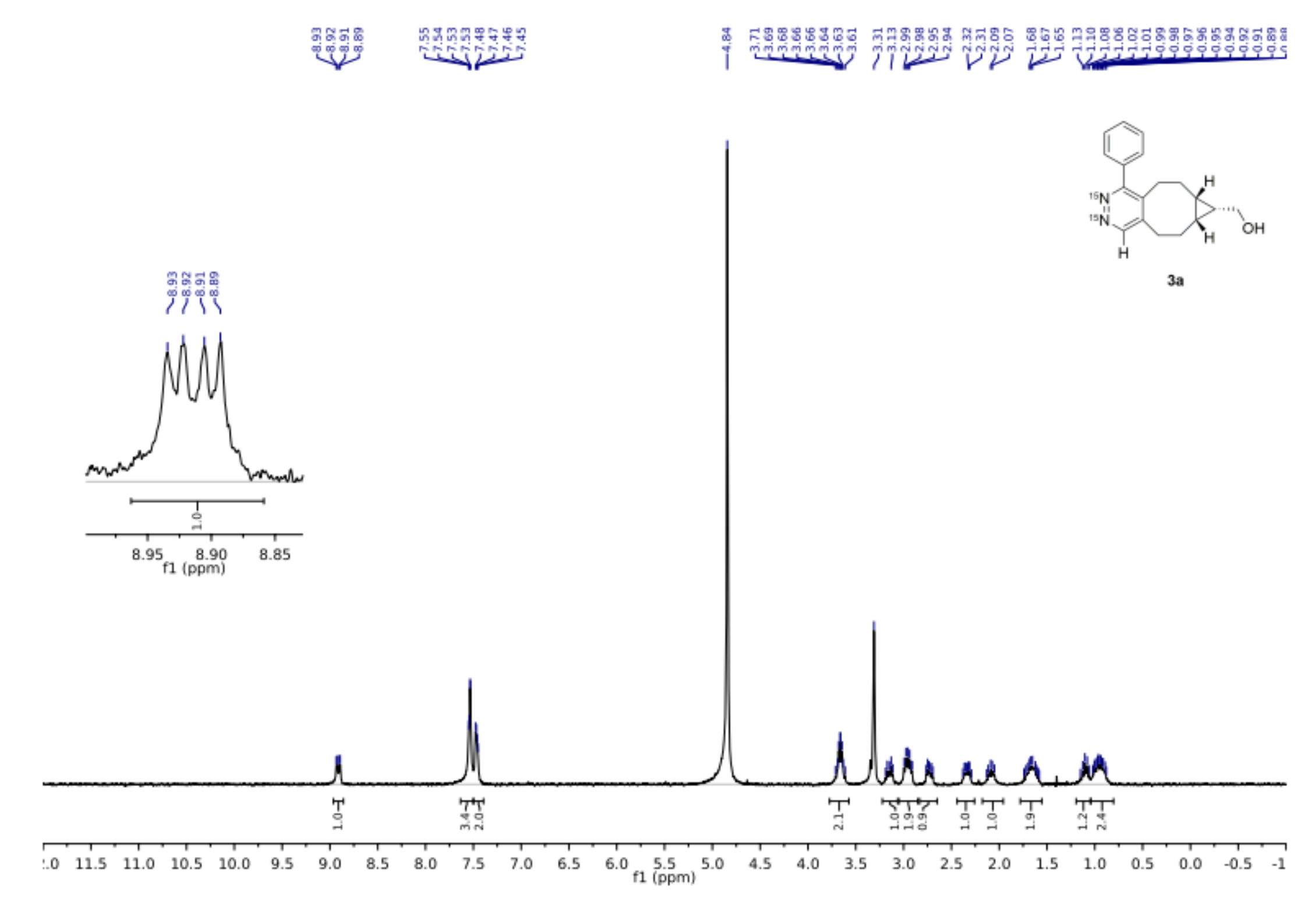
8.93
8.92
8.91
8.89
7.55
7.54
7.53
7.53
7.48
7.47
7.46
7.45
4.84
3.71
3.69
3.68
3.66
3.66
3.64
3.63
3.61
3.31
3.13
2.99
2.98
2.95
2.94
2.32
2.31
2.09
2.07
1.68
1.67
1.65
1.13
1.10
1.08
1.06
1.02
1.01
0.99
0.98
0.97
0.96
0.95
0.94
0.92
0.91
0.89
15N
15N
H
H
H
OH
3a
1.0
8.95
8.90
8.85
f1 (ppm)
1.0
3.4
2.0
2.1
1.0
1.9
0.9
1.0
1.0
1.9
1.2
2.4
f1 (ppm)

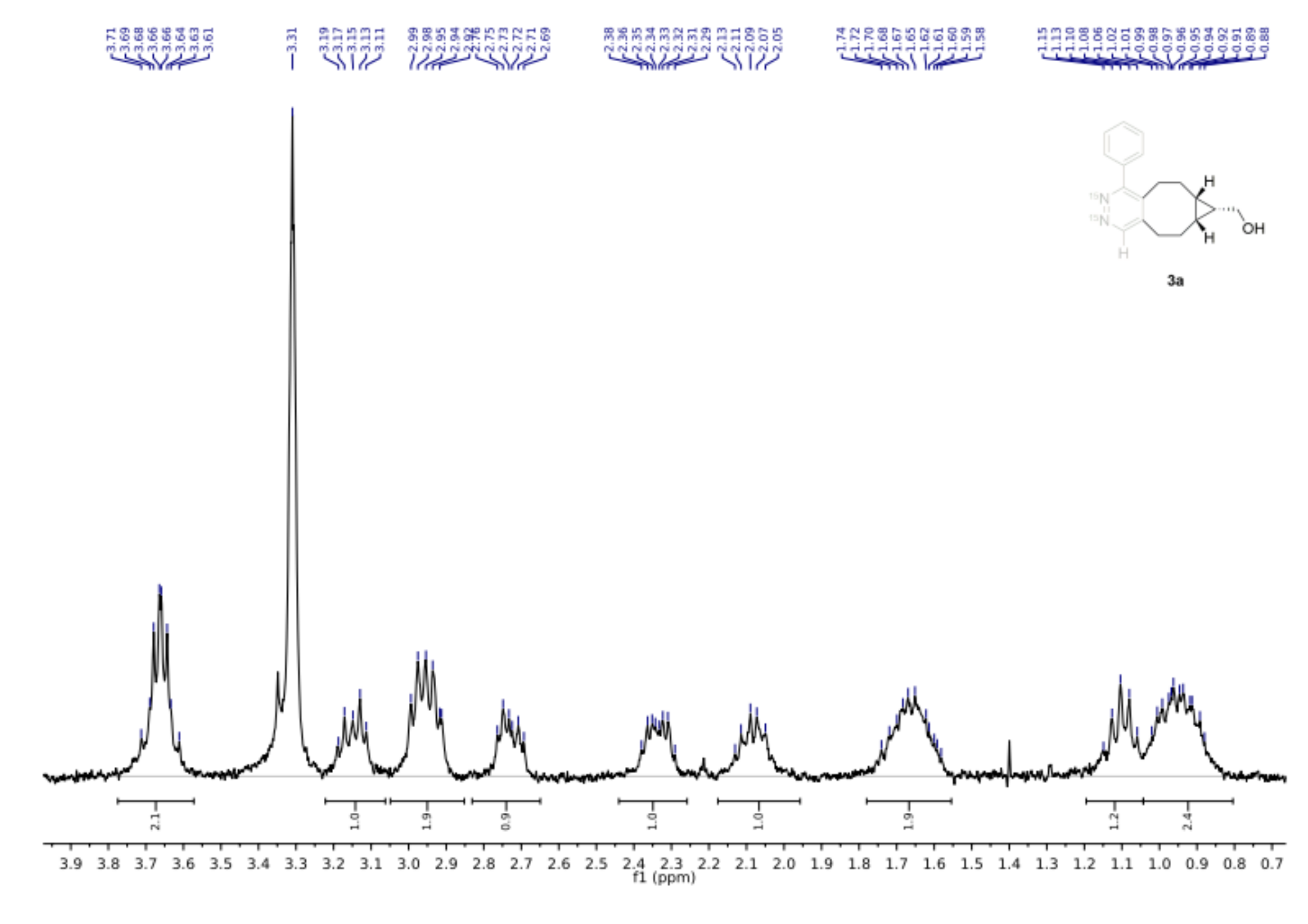
3.71 3.69 3.68 3.66 3.66 3.64 3.63 3.61
3.31
3.19 3.17 3.15 3.13 3.11
2.99 2.98 2.95 2.94 2.92 2.75 2.73 2.72 2.71 2.69
2.38 2.36 2.35 2.34 2.33 2.32 2.31 2.29 2.13 2.11 2.09 2.07 2.05
1.74 1.72 1.70 1.68 1.67 1.65 1.62 1.61 1.60 1.59 1.58
1.15 1.13 1.10 1.08 1.06 1.02 1.01 0.99 0.98 0.97 0.96 0.95 0.94 0.92 0.91 0.89 0.88
H
OH
H
H
3a
2.1
1.0
1.9
0.9
1.0
1.0
1.9
1.2
2.4
3.9 3.8 3.7 3.6 3.5 3.4 3.3 3.2 3.1 3.0 2.9 2.8 2.7 2.6 2.5 2.4 2.3 2.2 2.1 2.0 1.9 1.8 1.7 1.6 1.5 1.4 1.3 1.2 1.1 1.0 0.9 0.8 0.7
f1 (ppm)

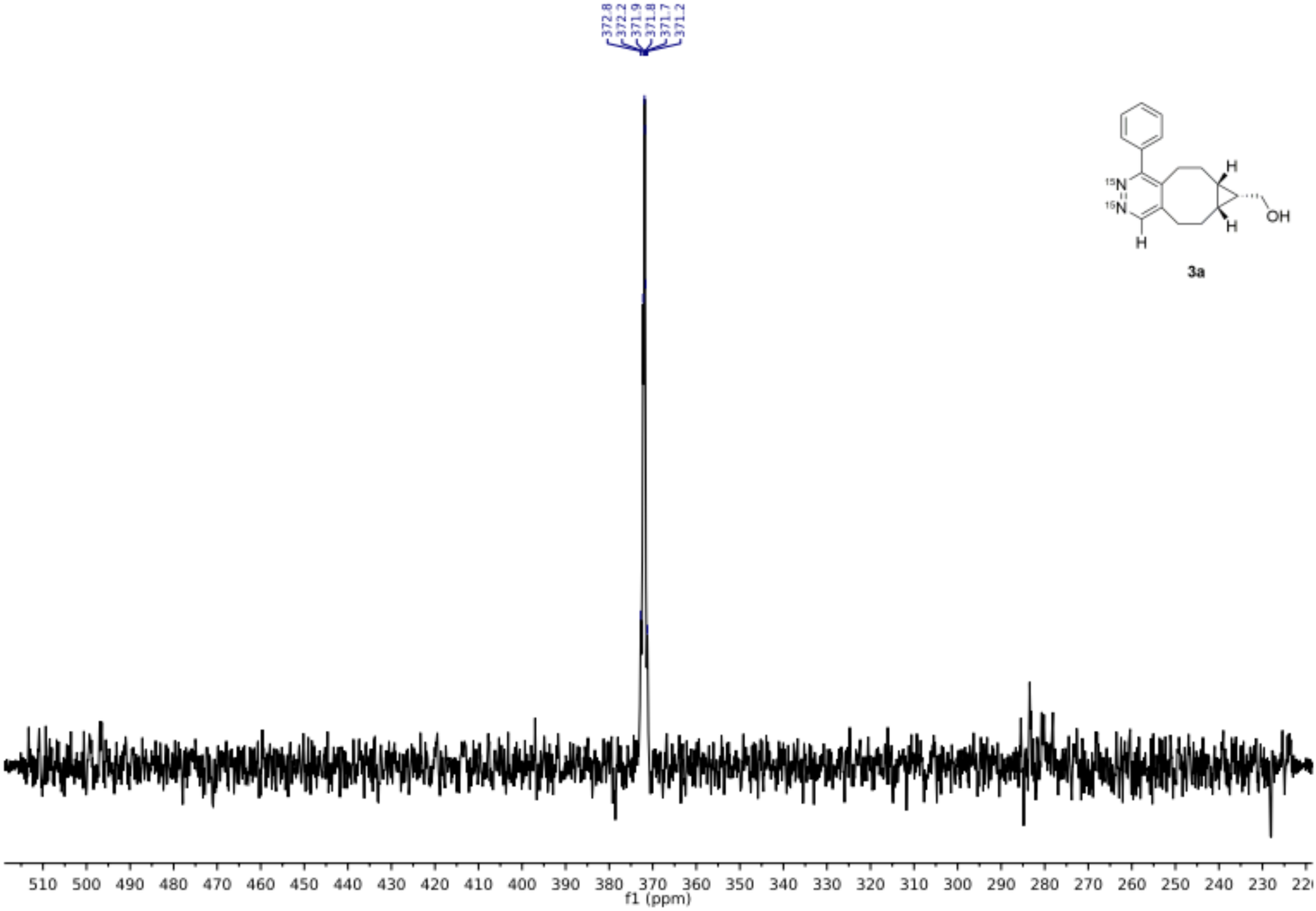
372.8
372.2
371.9
371.8
371.7
371.2
15N
15N
H
H
H
OH
3a
510 500 490 480 470 460 450 440 430 420 410 400 390 380 370 360 350 340 330 320 310 300 290 280 270 260 250 240 230
f1 (ppm)

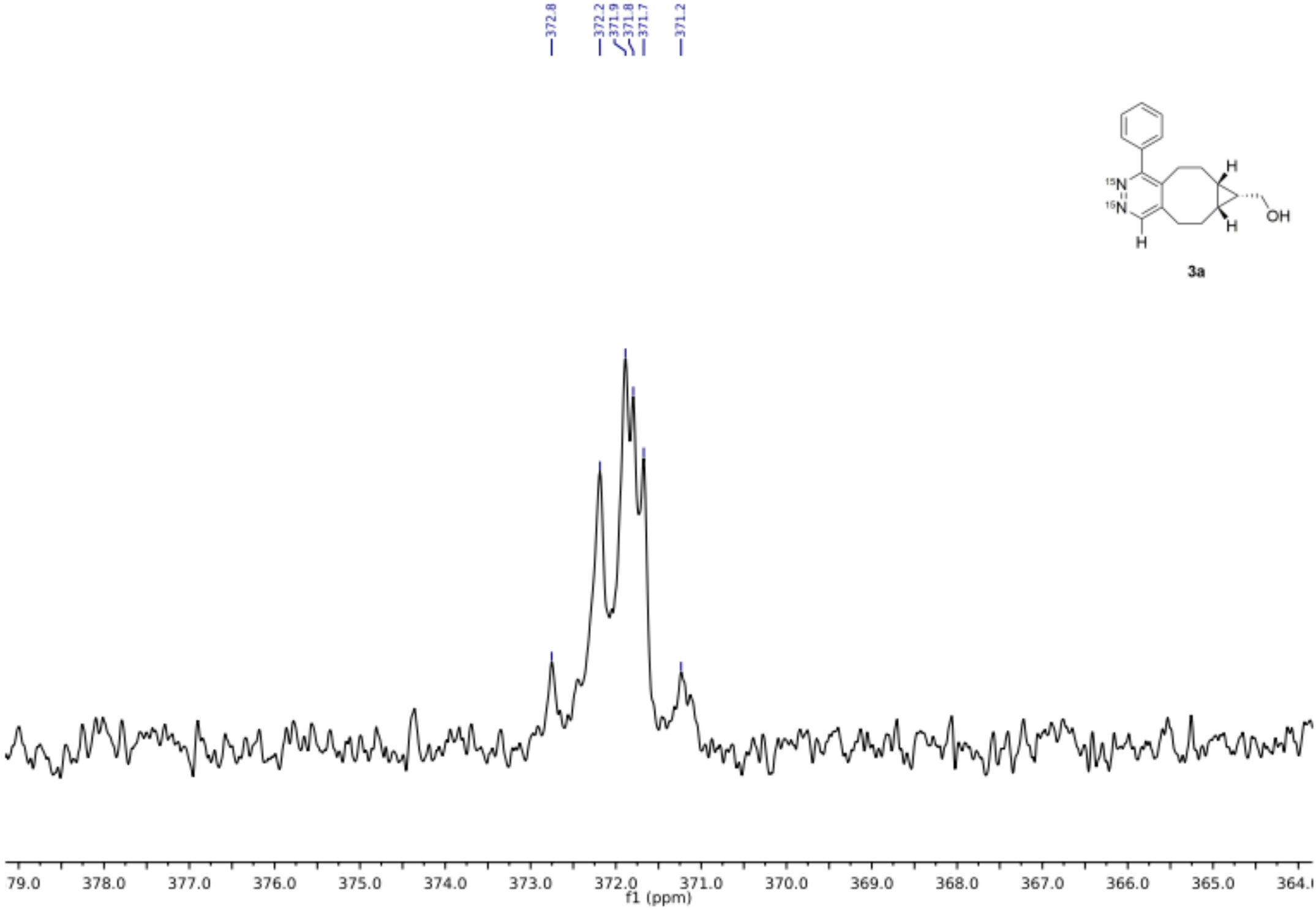
372.8
372.2
371.9
371.8
371.7
371.2
15N
15N
H
H
H
OH
3a
79.0
378.0
377.0
376.0
375.0
374.0
373.0
372.0
371.0
370.0
369.0
368.0
367.0
366.0
365.0
f1 (ppm)

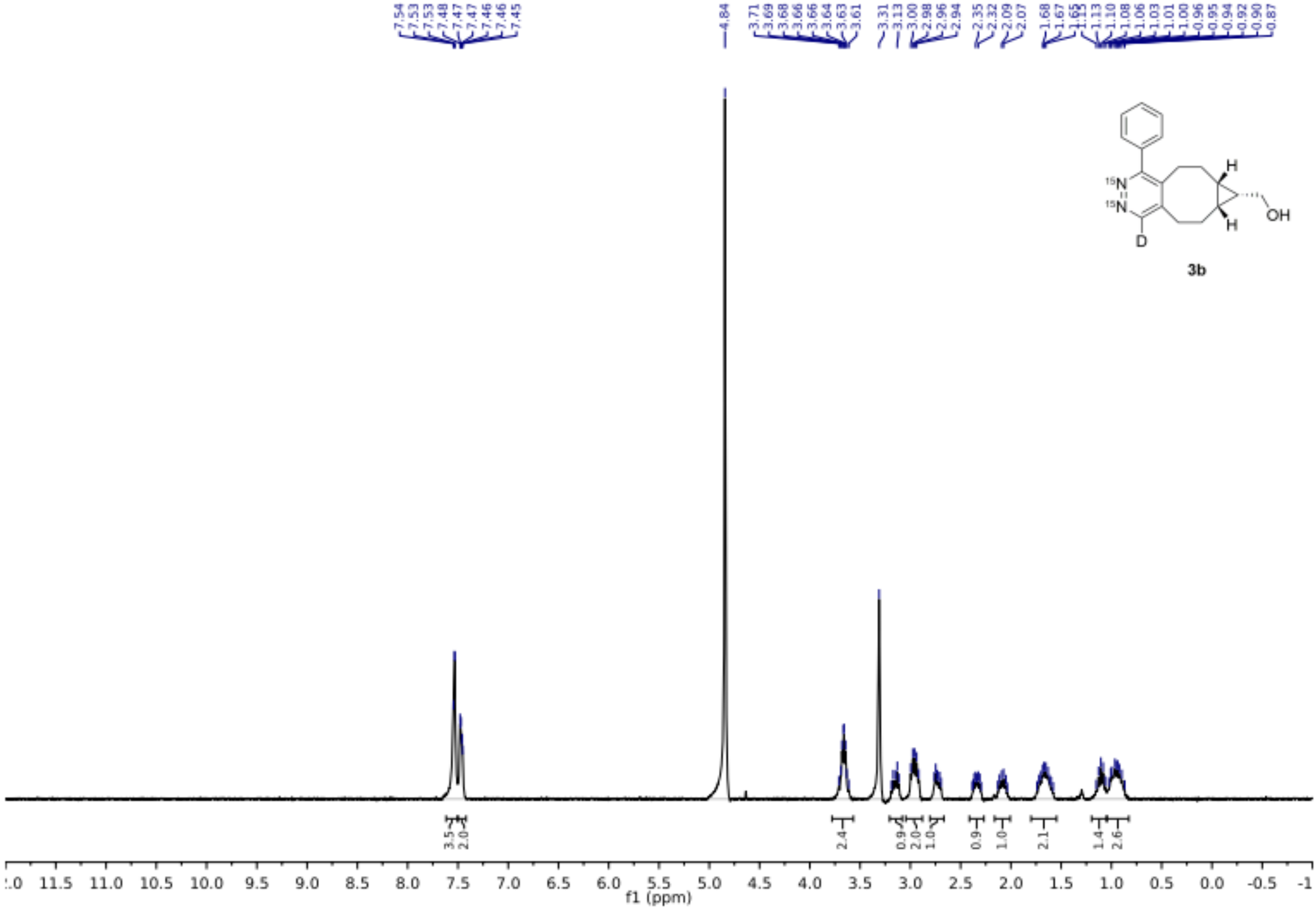
7.54
7.53
7.53
7.48
7.47
7.47
7.46
7.46
7.45
4.84
3.71
3.69
3.68
3.66
3.66
3.64
3.63
3.61
3.31
3.13
3.00
2.98
2.96
2.94
2.35
2.32
2.09
2.07
1.68
1.67
1.65
1.13
1.10
1.08
1.06
1.03
1.01
1.00
0.96
0.95
0.94
0.92
0.90
0.87
15N
15N
H
H
D
OH
3b
3.5
2.0
2.4
0.9
2.0
1.0
0.9
1.0
2.1
1.4
2.6
f1 (ppm)

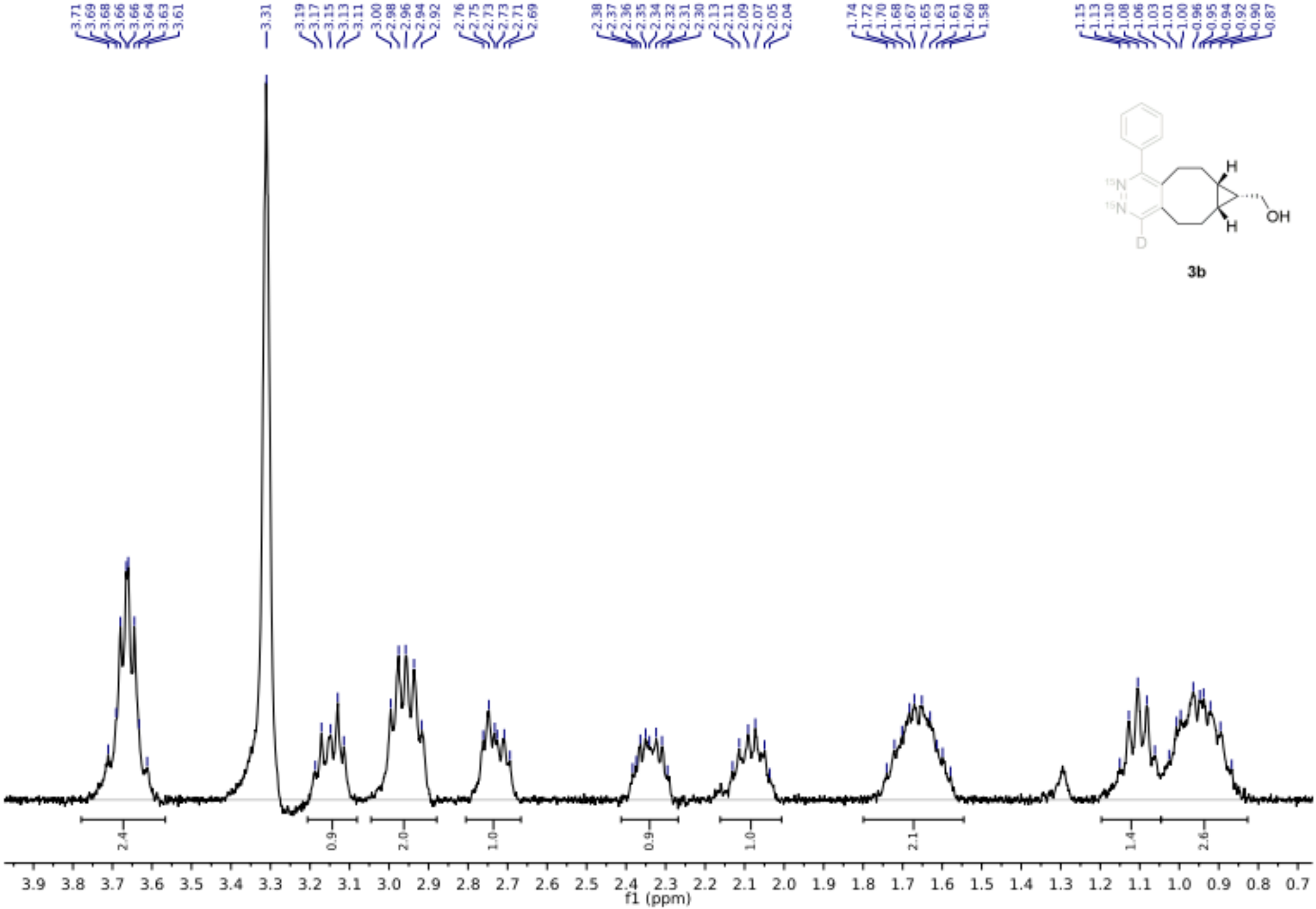
3.71 3.69 3.68 3.66 3.66 3.64 3.63 3.61
3.31
3.19 3.17 3.15 3.13 3.11
3.00 2.98 2.96 2.94 2.92
2.76 2.75 2.73 2.73 2.71 2.69
2.38 2.37 2.36 2.35 2.34 2.32 2.31 2.30
2.13 2.11 2.09 2.07 2.05 2.04
1.74 1.72 1.70 1.68 1.67 1.65 1.63 1.61 1.60 1.58
1.15 1.13 1.10 1.08 1.06 1.03 1.01 1.00 0.96 0.95 0.94 0.92 0.90 0.87
15N
15N
H
H
OH
D
3b
2.4
0.9
2.0
1.0
0.9
1.0
2.1
1.4
2.6
3.9 3.8 3.7 3.6 3.5 3.4 3.3 3.2 3.1 3.0 2.9 2.8 2.7 2.6 2.5 2.4 2.3 2.2 2.1 2.0 1.9 1.8 1.7 1.6 1.5 1.4 1.3 1.2 1.1 1.0 0.9 0.8 0.7
f1 (ppm)

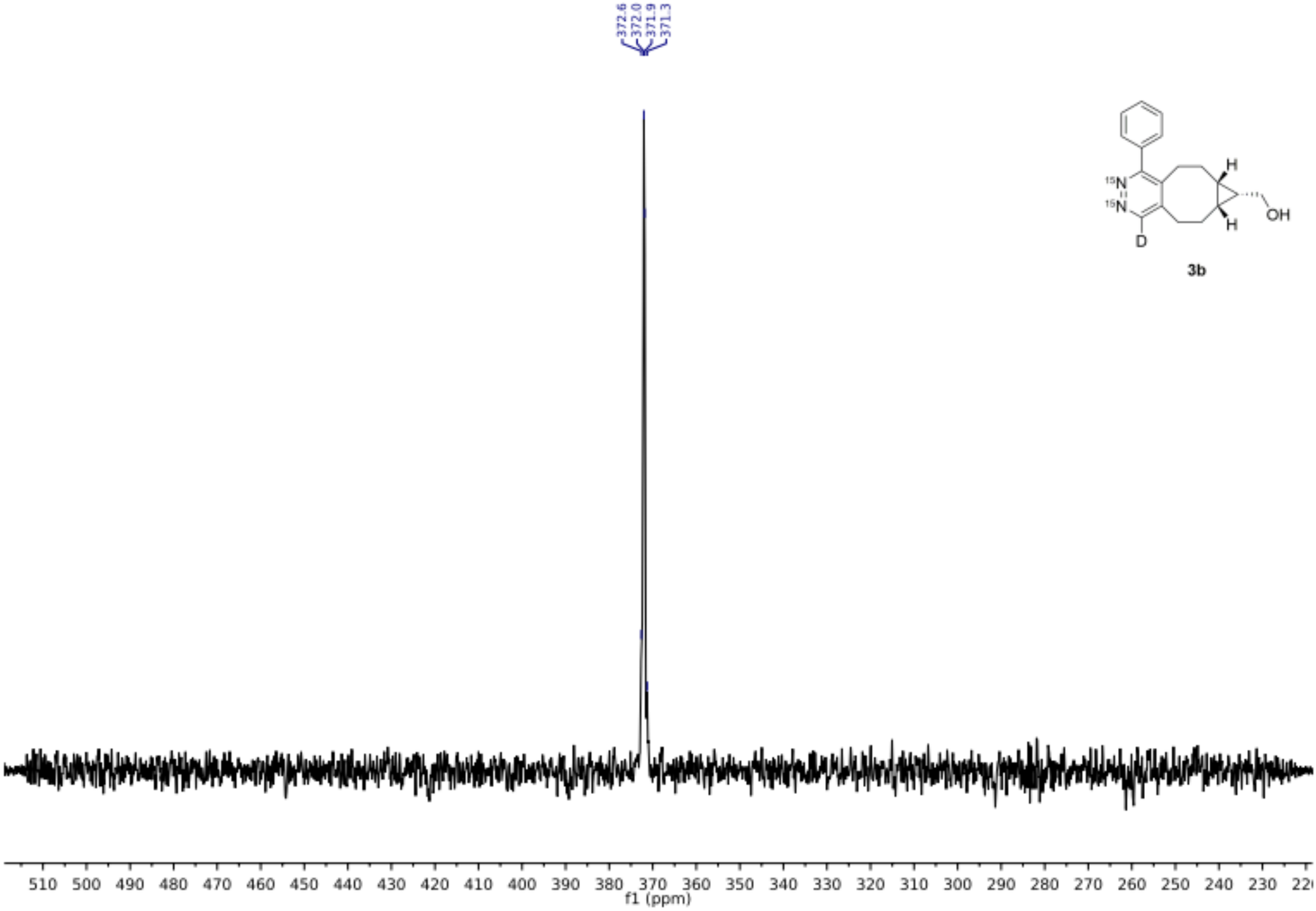
372.6
372.0
371.9
371.3
15N
15N
H
H
D
OH
3b
510 500 490 480 470 460 450 440 430 420 410 400 390 380 370 360 350 340 330 320 310 300 290 280 270 260 250 240 230
f1 (ppm)

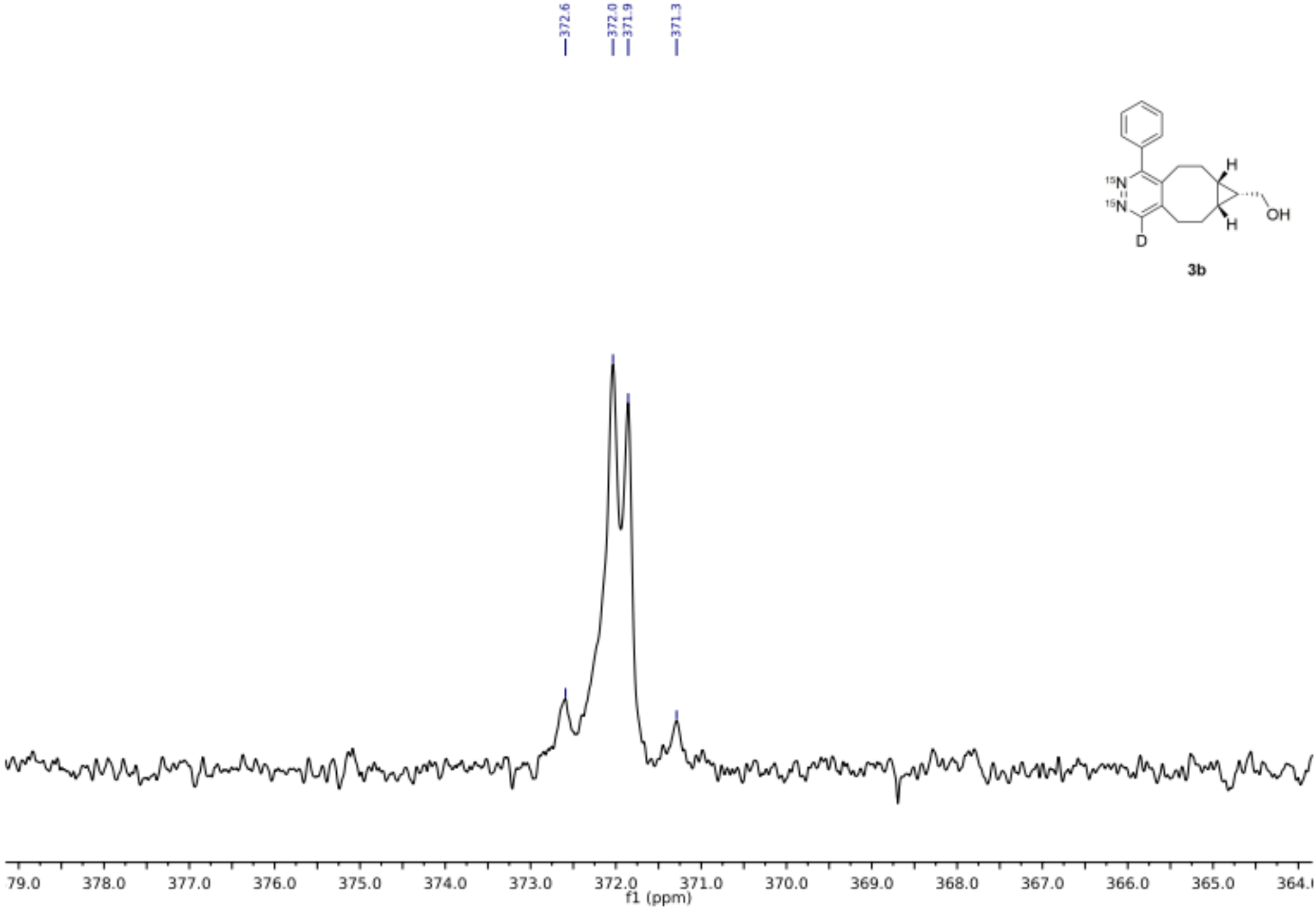
372.6
372.0
371.9
371.3
15N
15N
H
H
D
OH
3b
79.0
378.0
377.0
376.0
375.0
374.0
373.0
372.0
371.0
370.0
369.0
368.0
367.0
366.0
365.0
f1 (ppm)

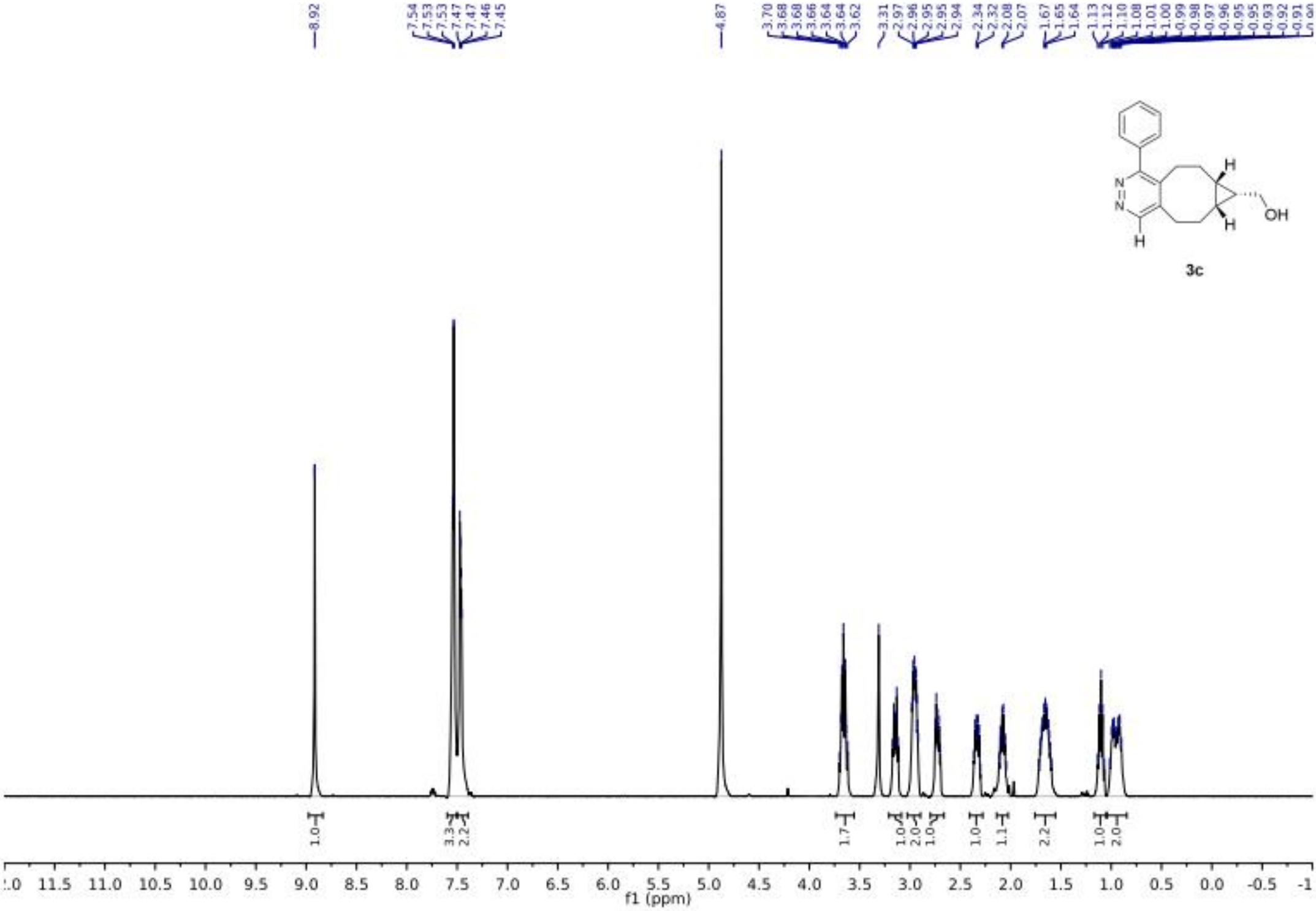
8.92
7.54
7.53
7.53
7.47
7.47
7.46
7.45
4.87
3.70
3.68
3.68
3.66
3.64
3.64
3.62
3.31
2.97
2.96
2.95
2.95
2.94
2.34
2.32
2.08
2.07
1.67
1.65
1.64
1.13
1.12
1.10
1.08
1.01
1.00
0.99
0.98
0.97
0.96
0.95
0.95
0.93
0.92
0.91
1.0
3.3
2.2
1.7
1.0
2.0
1.0
1.0
1.1
2.2
1.0
2.0
f1 (ppm)
N
N
H
H
H
OH
3c

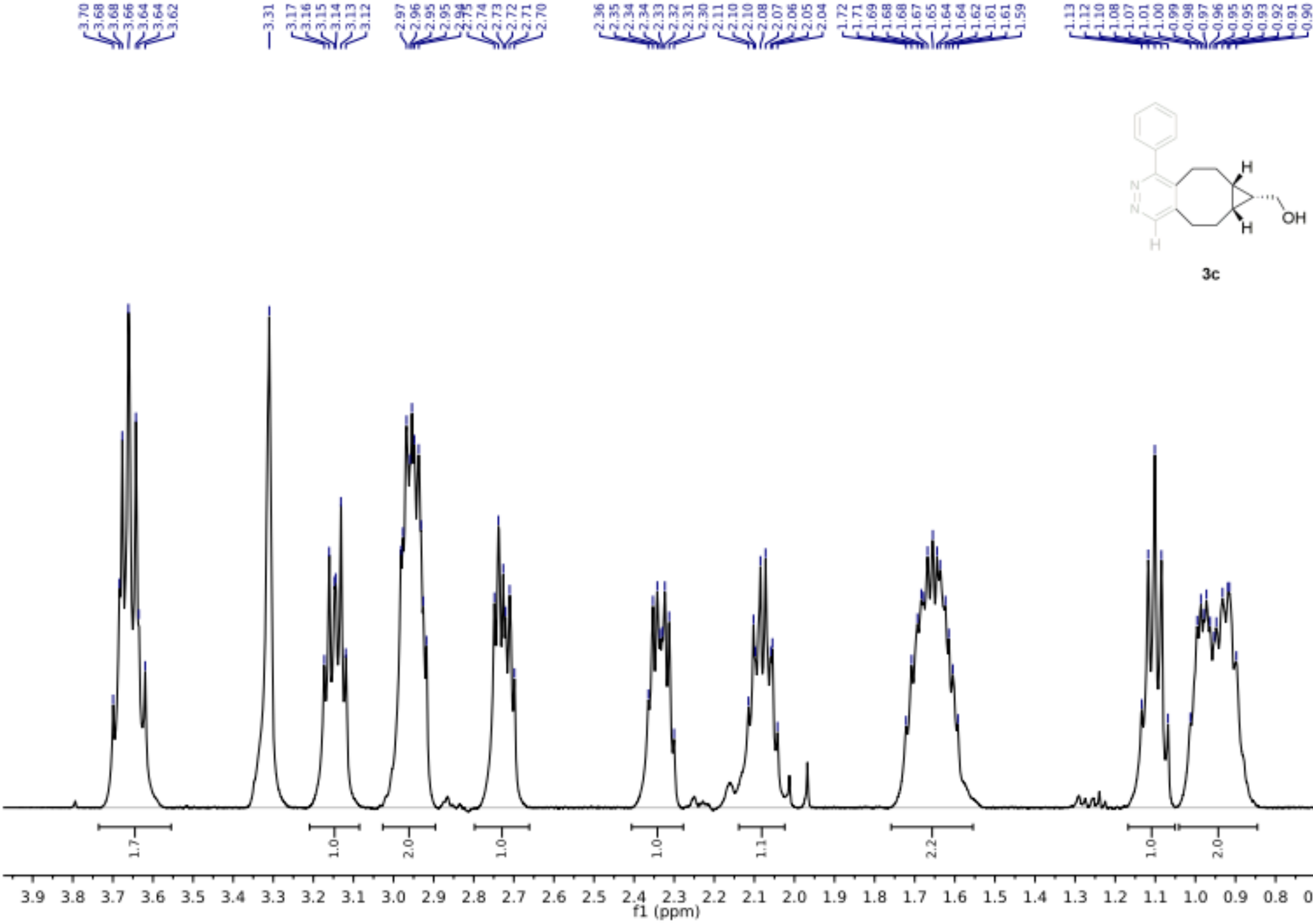
3.70 3.68 3.68 3.66 3.64 3.64 3.62
3.31
3.17 3.16 3.15 3.14 3.13 3.12
2.97 2.96 2.95 2.95 2.74 2.73 2.72 2.71 2.70
2.36 2.35 2.34 2.34 2.33 2.32 2.31 2.30
2.11 2.10 2.10 2.08 2.07 2.06 2.05 2.04
1.72 1.71 1.69 1.68 1.67 1.65 1.64 1.64 1.62 1.61 1.61 1.59
1.13 1.12 1.10 1.08 1.07 1.01 1.00 0.99 0.98 0.97 0.96 0.95 0.95 0.93 0.92 0.91 0.90
N
N
H
H
H
OH
3c
1.7
1.0
2.0
1.0
1.0
1.1
2.2
1.0
2.0
3.9 3.8 3.7 3.6 3.5 3.4 3.3 3.2 3.1 3.0 2.9 2.8 2.7 2.6 2.5 2.4 2.3 2.2 2.1 2.0 1.9 1.8 1.7 1.6 1.5 1.4 1.3 1.2 1.1 1.0 0.9 0.8 0.7
f1 (ppm)

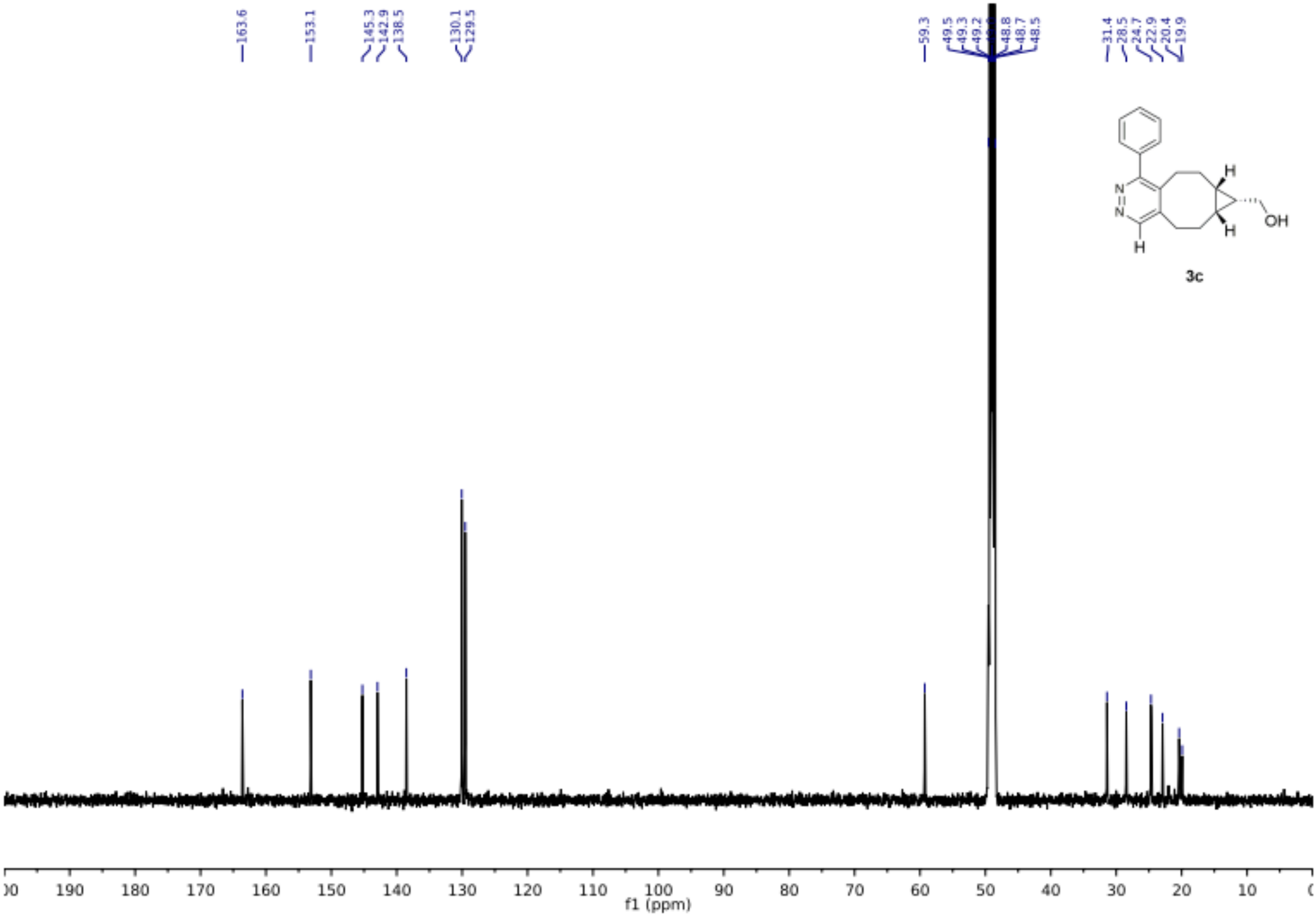
163.6
153.1
145.3
142.9
138.5
130.1
129.5
59.3
49.5
49.3
49.2
48.8
48.7
48.5
31.4
28.5
24.7
22.9
20.4
19.9
N
N
H
H
H
OH
3c
f1 (ppm)

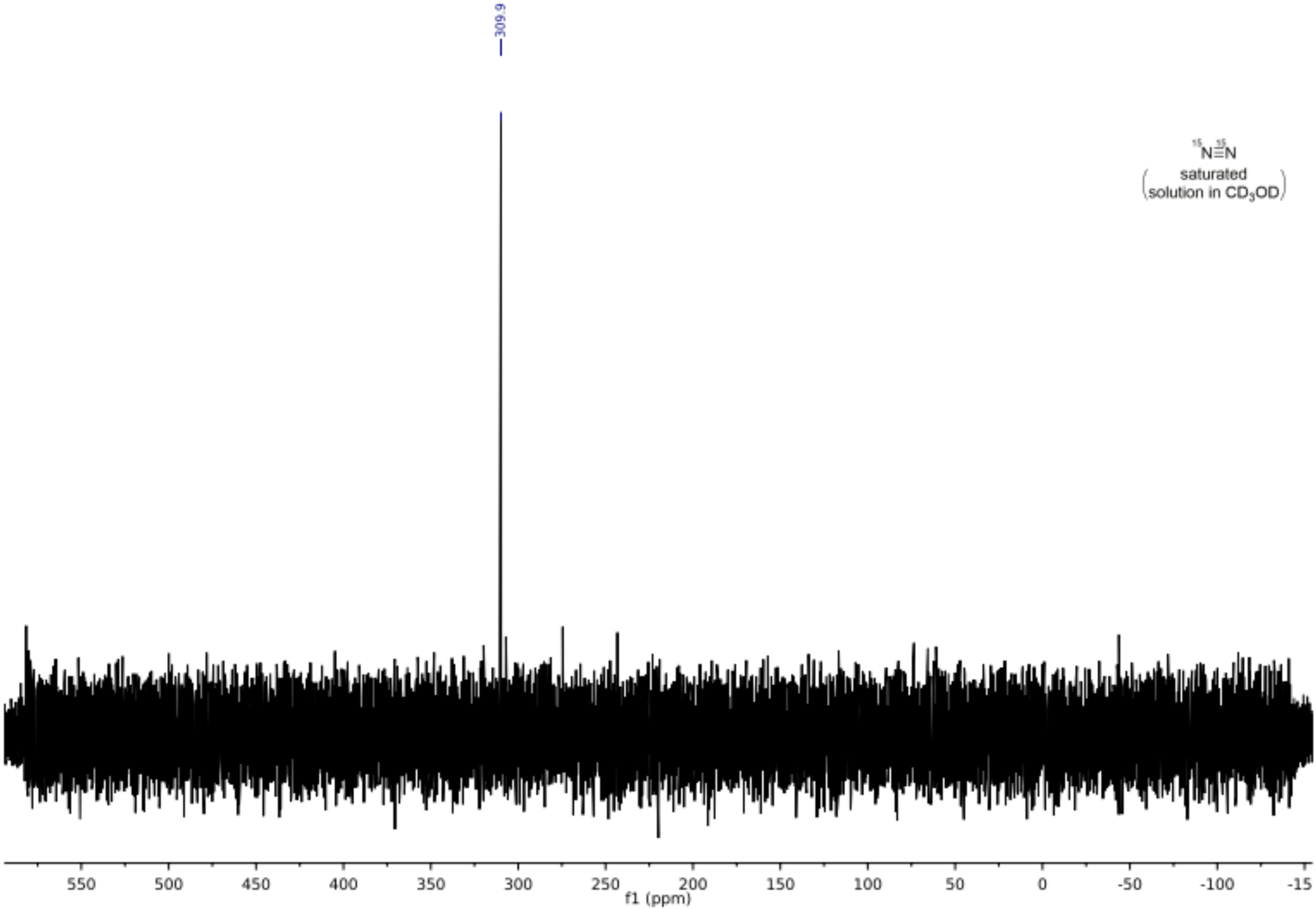
309.9
$^{15}N\equiv{}^{15}N$
saturated
solution in CD_3OD
550
500
450
400
350
300
250
200
150
100
50
0
-50
-100
-15
f1 (ppm)

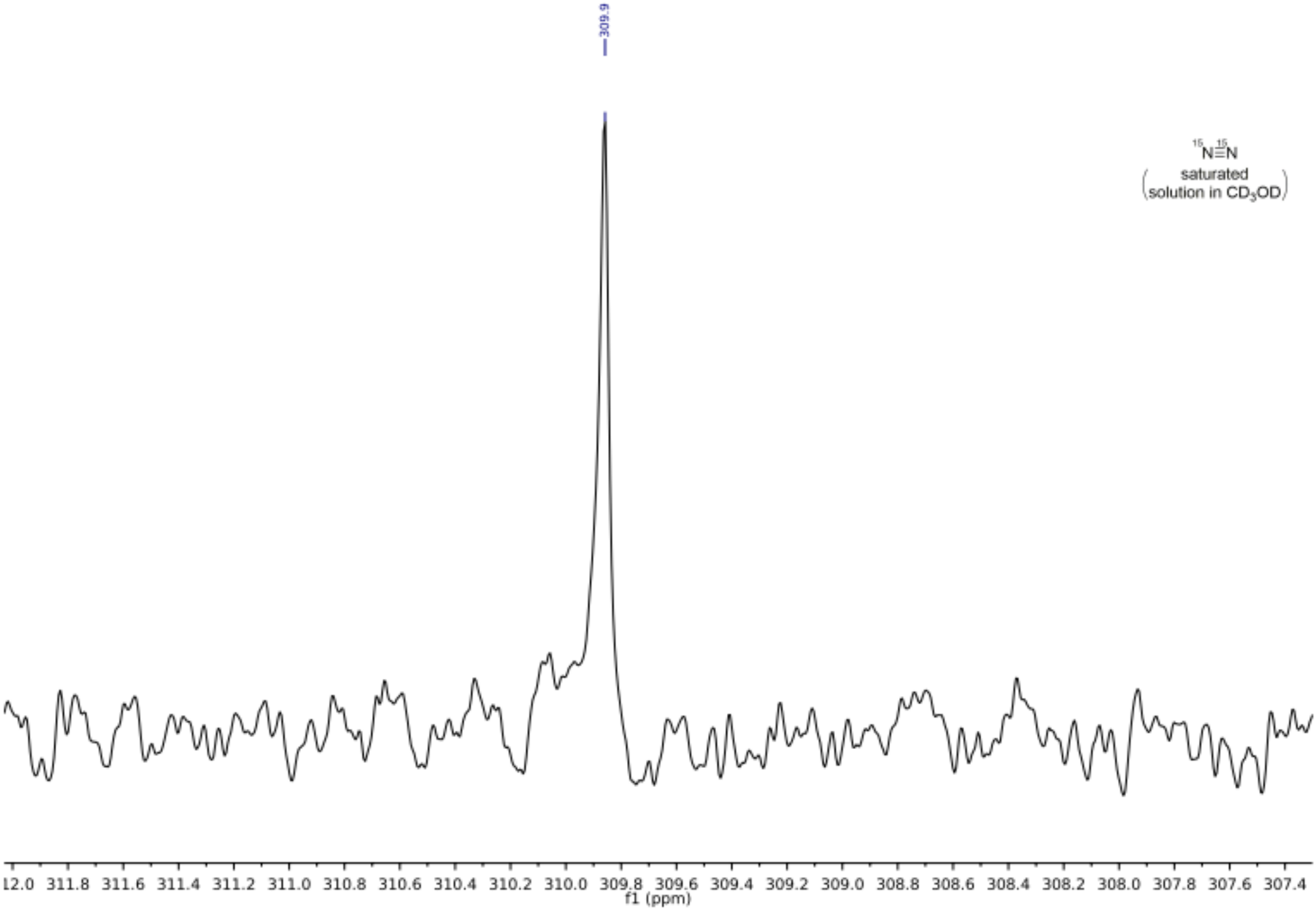
309.9
$^{15}N\equiv{}^{15}N$
saturated
(solution in CD_3OD)
312.0 311.8 311.6 311.4 311.2 311.0 310.8 310.6 310.4 310.2 310.0 309.8 309.6 309.4 309.2 309.0 308.8 308.6 308.4 308.2 308.0 307.8 307.6 307.4
f1 (ppm)